



Efficiency Improvement of Permanent Magnet Synchronous Motors and Generators

A. O. Di Tommaso



The present work will demonstrate first that efficiency improvement of PMSMachines can be achieved by acting:

- 1) on the control strategy;
- 2) on the machine design (by choosing suitable geometries, materials, winding, etc.);
- 3) the machine design procedure can be used for both motors and generators;
- 4) finally a possible application for small wind power turbines is proposed.



Permanent magnet synchronous motors (PMSMs) fed by inverters are widely used in industrial applications for their high performances. Main advantages are:

- Higher efficiency and higher power-weight ratio than dc and induction motors.
- Loss-free rotor, and the power losses are mainly related to the stator windings and the stator core.
- The ratio of the copper and iron power losses is a key issue in determining the maximum efficiency



- A control algorithm is presented, which is able to improve the efficiency of permanent magnet synchronous motor drives by reducing the motor losses (copper and iron losses) through an optimal management of the current space vector in the stator winding.
- The control algorithm here proposed allows determining the optimal current space vector according to the operating speed and the load conditions.
- The test results have shown that its dynamic performances are maintained, and enhancement of the efficiency up to 3% can be reached in comparison to a PMSM drive equipped with a traditional control strategy (i.e. $i_d=0$).



State of the Art

- Control techniques can be summarized into two main categories:
 - “loss model control” technique
 - “search control” technique
- The “loss model control” technique is based on the development of a mathematical model, which allows to estimate the energy losses occurring during the running of the motor.
- The “search control” algorithm, on the contrary, is not based on a model rather on an adaptive routine.



Loss Minimization Techniques:



State of the Art

The “Loss model control” requires the knowledge of a precise system model, an accurate identification of its parameters, and also the variation of the parameters with the temperature, current, etc.

By expressing the losses as a function of the control variables of the drive it is possible to impose an operating condition to obtain the maximum efficiency.



Loss Minimization Techniques:



State of the Art

The “Search Control” technique: is based on changing step by step the value of a control variable, then measuring for each operating point the active power flowing into the motor; next, by comparing the measurement result with the previous one at fixed operating conditions, the minimum power consumption of the drive is searched.

The “search control” algorithm has the advantage that there is no need to know the model of the motor and its parameters.

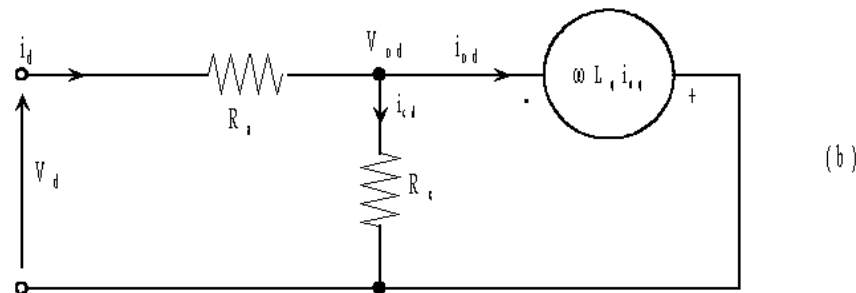
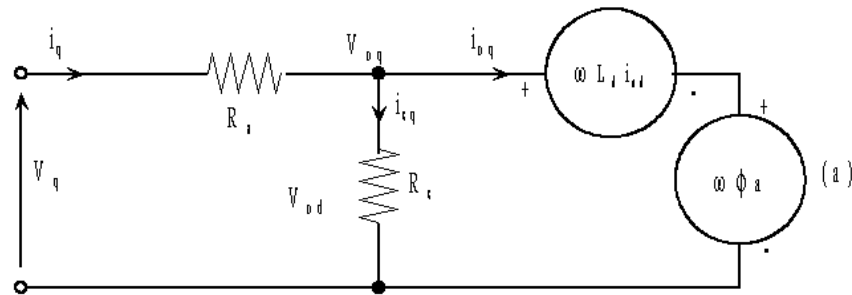
A drawback is that such a technique can originate system oscillation phenomena (instability of the drive).



Loss Minimization Techniques:

State of the Art

By considering the two-axes theory of Park and introducing a resistance R_c in the model to account for the iron losses, the dynamic d- and q-axis equivalent circuits of the PMSM can be drawn, as it is shown in the figure.



The power losses in a PMSM are divided in:

Copper losses;

Iron losses;

Mechanical losses;

Additional iron and copper losses;

1) and 2) belong to the “controllable” losses;

3) and 4) belong to the “uncontrollable” ones;



Loss Minimization Algorithm

Manipulating the mathematical model and by setting to zero its time derivatives the expressions of the copper and iron losses are obtained.

$$W_{\text{copper}} = \int_{t_0}^{t_1} \left(\frac{1}{2} R_{\text{copper}} i^2 \right) dt$$

$$W_{\text{iron}} = \int_{t_0}^{t_1} \left(\frac{1}{2} R_{\text{iron}} i^2 \right) dt$$

$$W_{\text{total}} = \int_{t_0}^{t_1} \left(\frac{1}{2} R_{\text{copper}} i^2 + \frac{1}{2} R_{\text{iron}} i^2 \right) dt$$

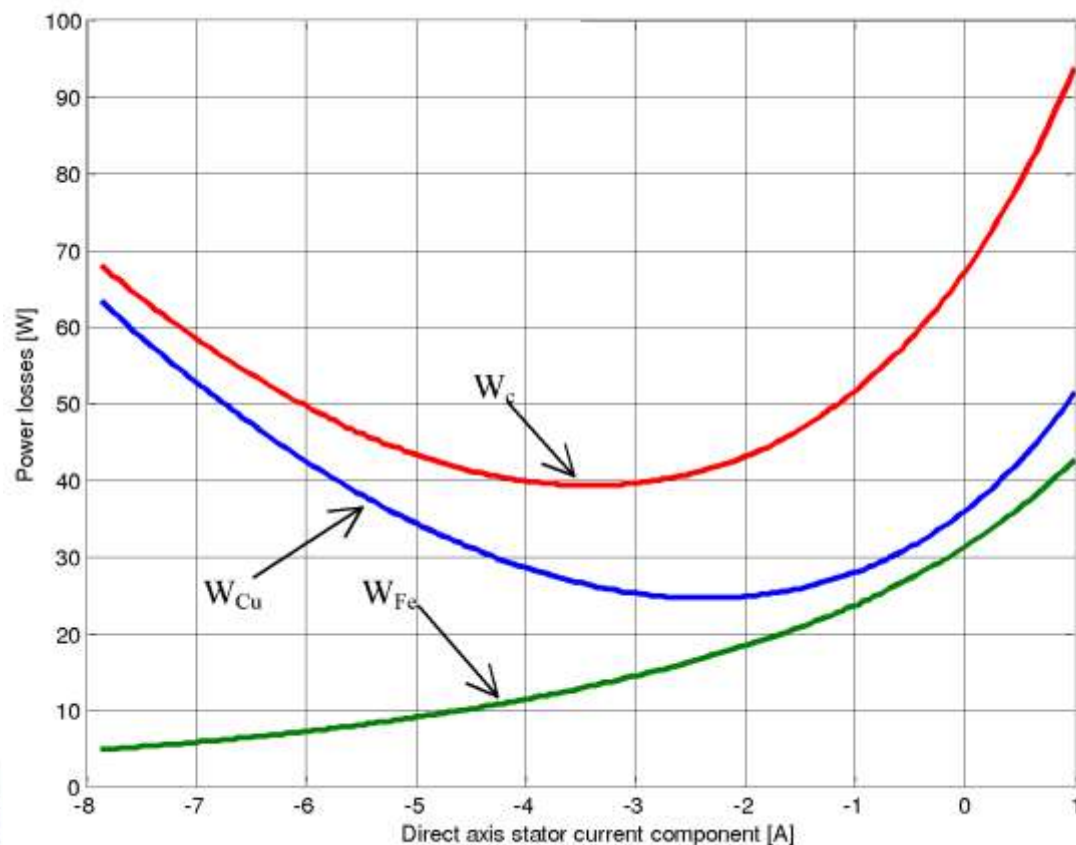


Loss Minimization Algorithm

Combining the previous relations the power losses of the motor as function of T_e , i_{od} and ω_r is obtained:

$$P_{loss} = P_{cu} + P_{fe} + P_{c} + P_{mech}$$

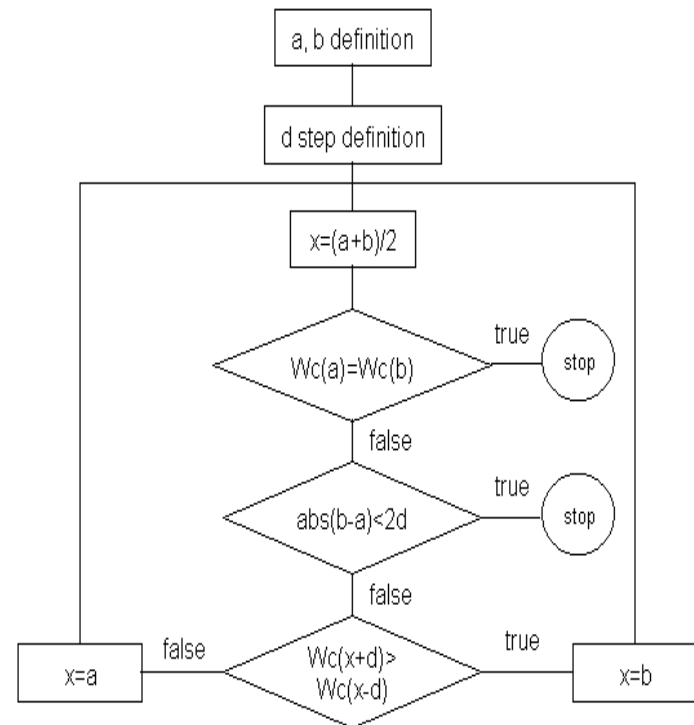
Electrical power losses as a function of the direct axis current component i_{od} at rated speed and rated load.



Loss Minimization Algorithm

- The determination of the minimum power loss can be pursued by adopting an iterative numerical algorithm.
- In this case an interval-reduction algorithm has been chosen, being it a useful and highly efficient calculation procedure for all those functions that present in the searching interval only a local minimum

Flow chart of the minimization algorithm. a and b are the search interval limits, d is the search step, x the medium test point of the interval (a, b) , $W_c(x)$ are the power losses.



Loss Minimization Algorithm



```
double a, b, Lambda, sep, Ld, Lq, R, Rc, p, xl, xr, xmax, ioq, ioql, ioqr, WCU, WCul, WCur, WFe, WFeL, WFeR, Wt, WtL, Wtr, T, w;  
  
T = u[0];  
w = u[1];  
a = *param0;  
b = *param1;  
sep = *param2;  
Lambda = *param3;  
Ld = *param4;  
Lq = *param5;  
R = *param6;  
Rc = *param7;  
p = *param8;  
  
do {  
xl = a + 0.5 * (b - a - sep);  
xr = xl + sep;  
ioql = T / (1.5 * p * (Lambda + (Ld - Lq) * xl));  
WCul = 1.5 * R * (pow((xl - p * w * Lq * ioql / Rc),2) + pow((ioql + p * w * (Lambda + Ld * xl) / Rc),2));  
WFeL = 1.5 / Rc * (pow((p * w * Lq * ioql),2) + pow((p * w * (Lambda + Ld * xl)),2));  
WtL = WCul + WFeL;  
  
ioqr = T / (1.5 * p * (Lambda + (Ld - Lq) * xr));  
WCur = 1.5 * R * (pow((xr - p * w * Lq * ioqr / Rc),2) + pow((ioqr + p * w * (Lambda + Ld * xr) / Rc),2));  
WFeR = 1.5 / Rc * (pow((p * w * Lq * ioqr),2) + pow((p * w * (Lambda + Ld * xr)),2));  
Wtr = WCur + WFeR;  
  
if (WtL <= Wtr) { b = xr; }  
if (Wtr < WtL) { a = xl; }  
}  
while (!(WtL == Wtr) || ((b - a) <= (2 * sep)));  
  
xmax = 0.5 * (xl + xr);  
ioq = T / (1.5 * p * (Lambda + (Ld - Lq) * xmax));  
WCU = 1.5 * R * (pow((xmax - p * w * Lq * ioq / Rc),2) + pow((ioq + p * w * (Lambda + Ld * xmax) / Rc),2));  
WFe = 1.5 / Rc * (pow((p * w * Lq * ioq),2) + pow((p * w * (Lambda + Ld * xmax)),2));  
Wt = WCU + WFe;  
y[0] = xmax - p * w * Lq * ioq / Rc; /* id */  
y[1] = ioq + (p * w * (Lambda + Ld * xmax)) / Rc; /* iq */
```



18 November 2010
University of Palermo



The Test Bench

- A comparison has been made between two different approaches: the loss minimization algorithm (LMA) discussed in the previous slides, and a traditional $i_d=0$ control.
- The parameters of the simulated PMSM (1 kW motor drive) are listed in Table I.

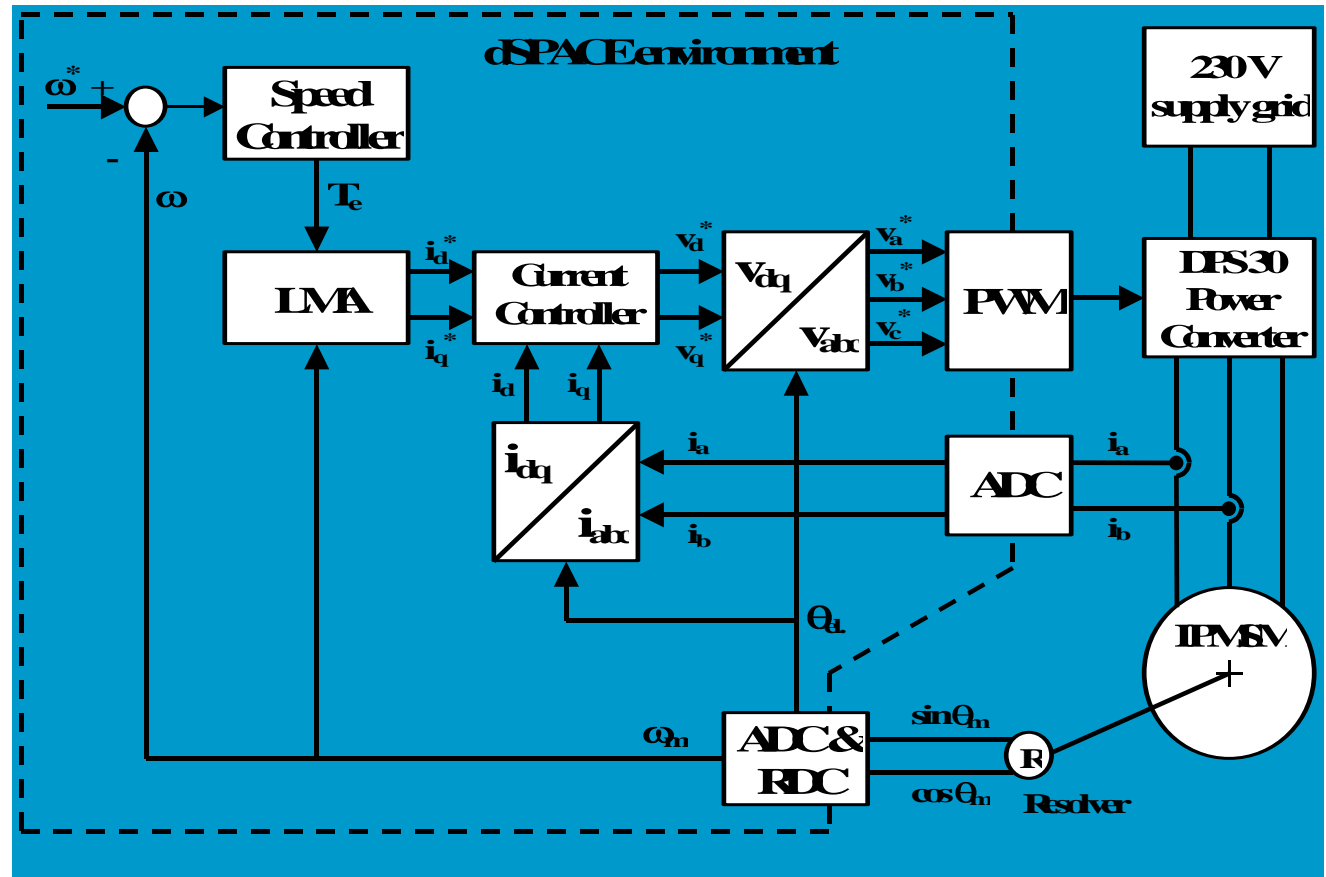
Table 1. Nameplate data and per phase parameters values of a PMSM.

Rated speed [rpm]	4000
Rated current (rms) [A]	3.6
Rated torque [Nm]	1.8
Number of poles	6
Armature resistance R [ohm]	2.21
Equivalent resistance of the iron losses R_c [ohm]	840
Direct axis inductance [mH]	9.77
Quadrature axis inductance [mH]	14.94
Permanent magnet flux [Wb]	0.0844
Mechanical losses (torque) [Nm]	0.04



The Test Bench

Simplified schematic of the PMSM drive (LMFOC)

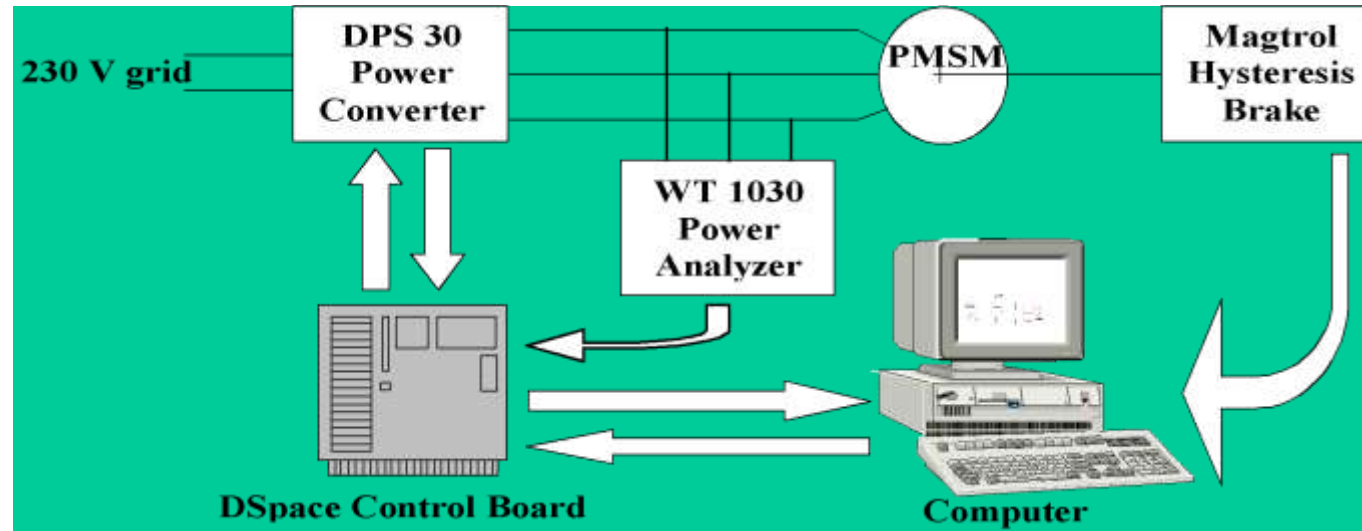


The Test Bench

Input voltage (single phase) [V]	230
Motor supply rail (VDC) [V]	310
Output power peak [kW]	6.5
Phase current peak (crest) [A]	30
Phase current cont. (RMS) [A]	21
Switching frequency [kHz]	5÷20
Shunt power peak [W]	3200

Table 2. Electrical characteristics of the IGBT power converter

Simplified schematic of the PMSM drive test bench

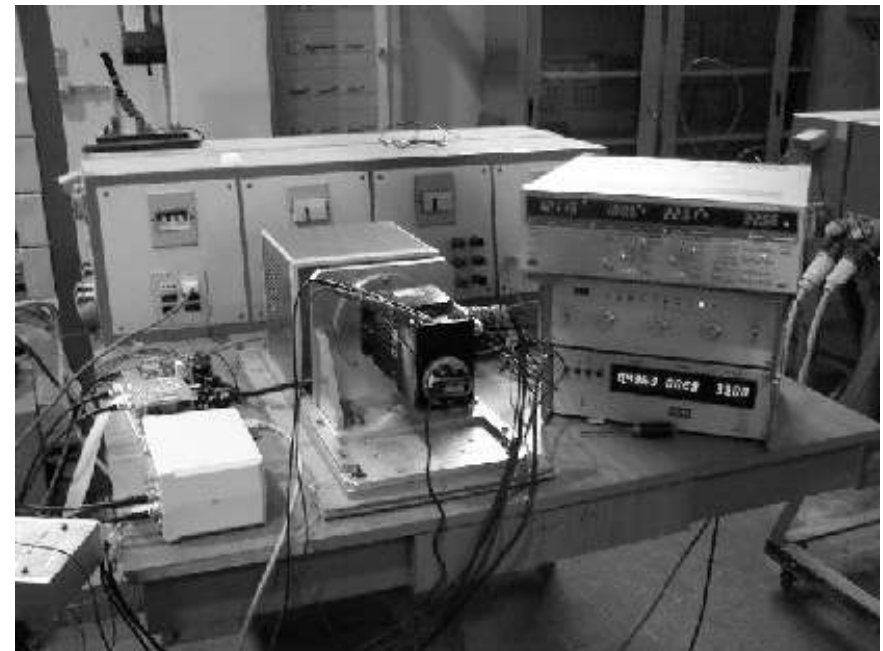
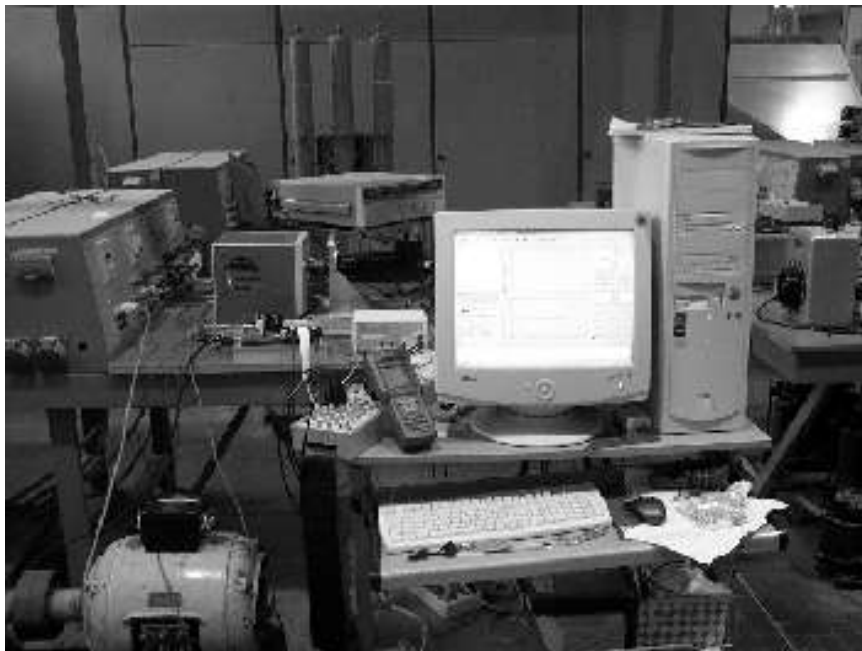


18 November 2010
University of Palermo



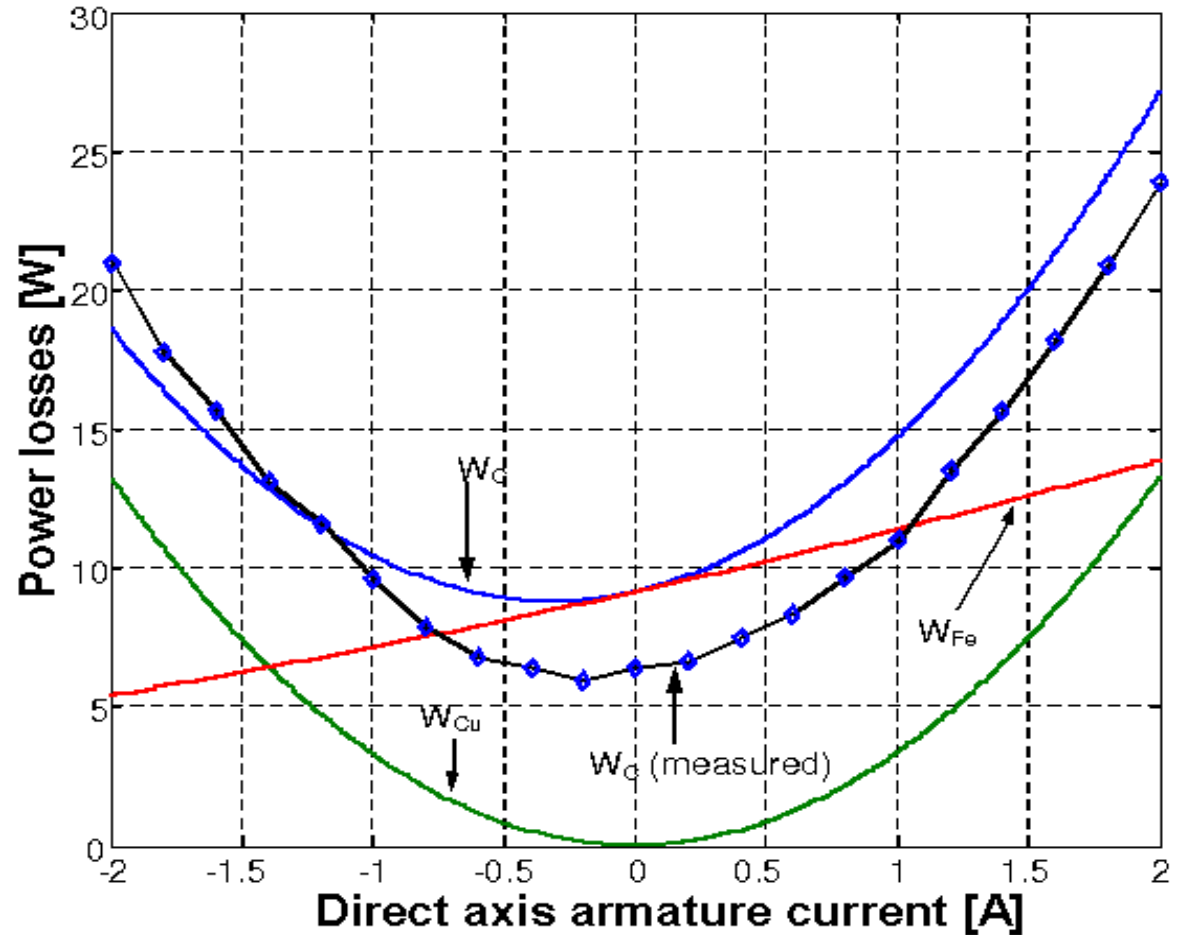
The Test Bench

The test bench particular of the PMSM with the converter, the controlled brake and the power analyzer.



Laboratory Test Results

Estimated and measured power losses of the test motor at 3000 rpm and no load condition.

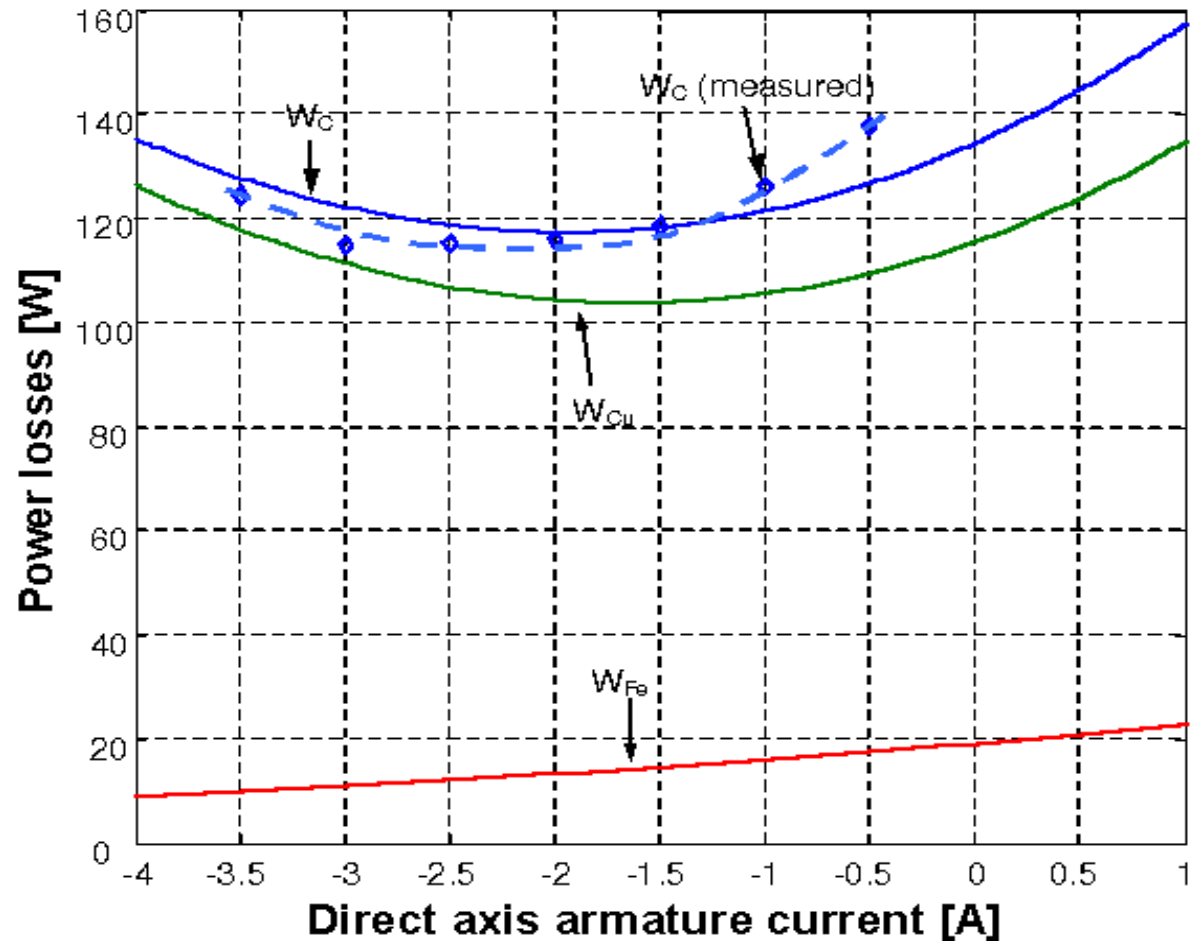


18 November 2010
University of Palermo



Laboratory Test Results

Estimated and measured power losses of the test motor at 3000 rpm and full load condition.

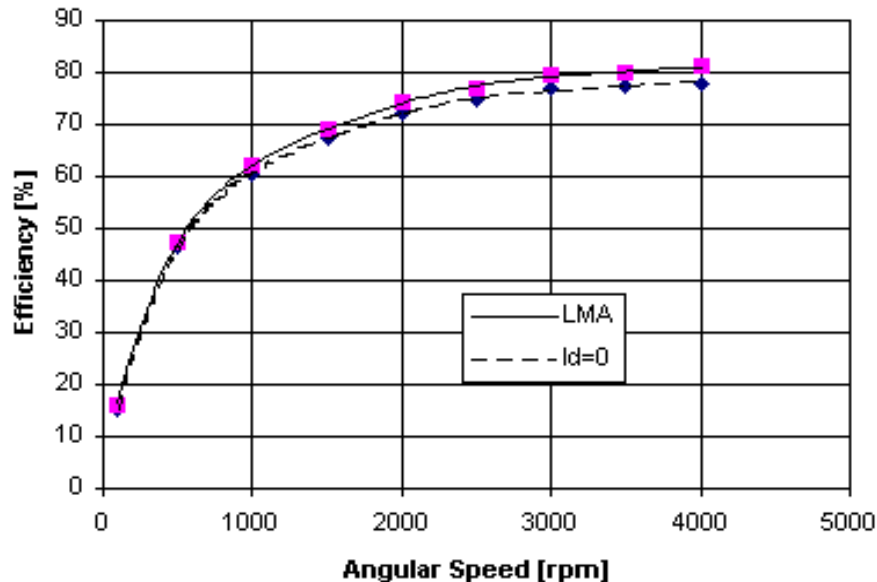


18 November 2010
University of Palermo

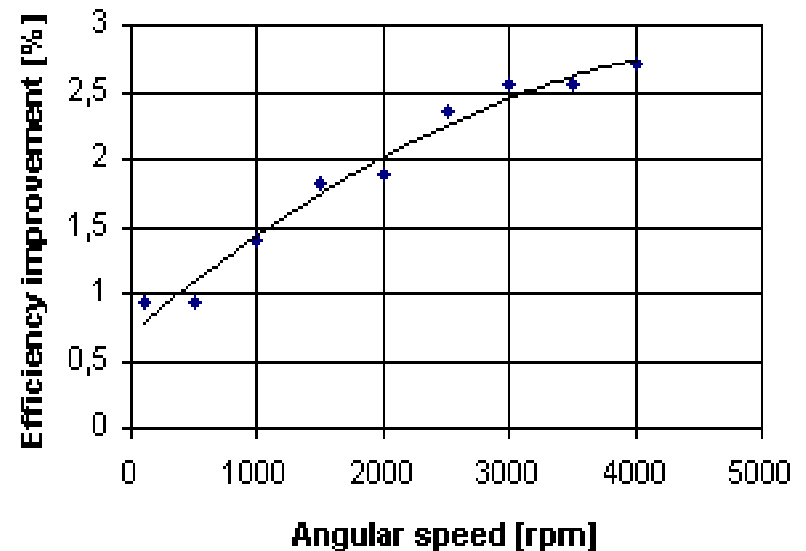


Laboratory Test Results

Comparison of the motor efficiencies at rated load (1.8 Nm) vs. the angular speed (rpm) in the case of LMA (continuous curve) and of $i_d = 0$ (dotted curve) controls.

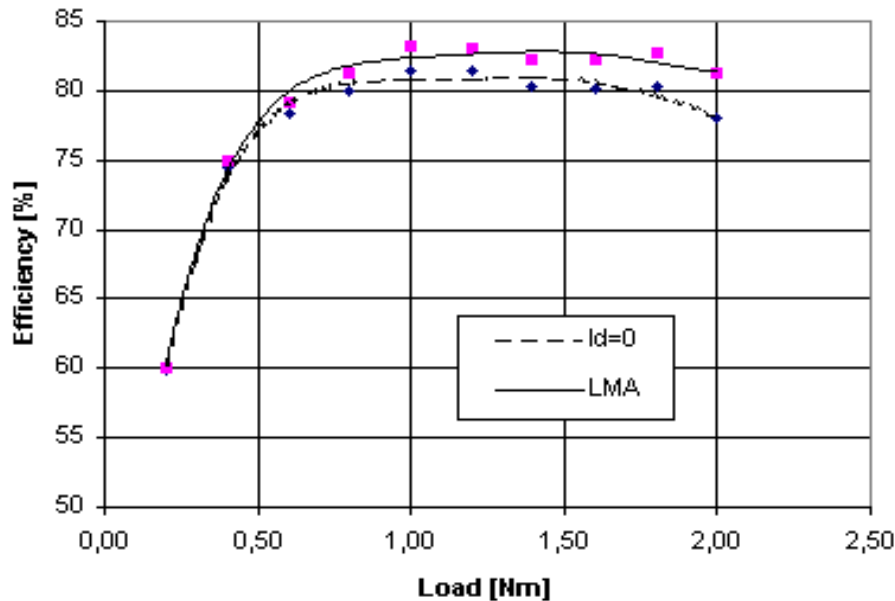


Achievable efficiency improvement due to LMA (referred to the traditional control approach) versus the angular speed at rated load condition (1.8 Nm).

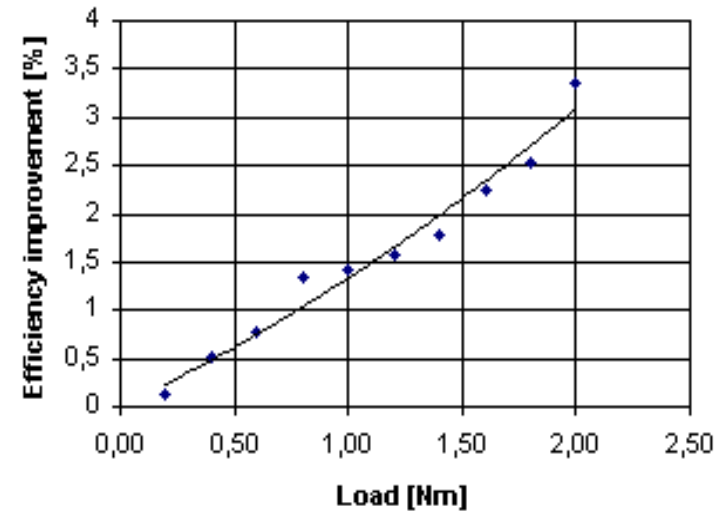


Laboratory Test Results

Comparison of the motor efficiencies at rated speed (4000 rpm) versus the load torque in the case of LMA (continuous curve) and of $i_d=0$ (dotted curve) controls.

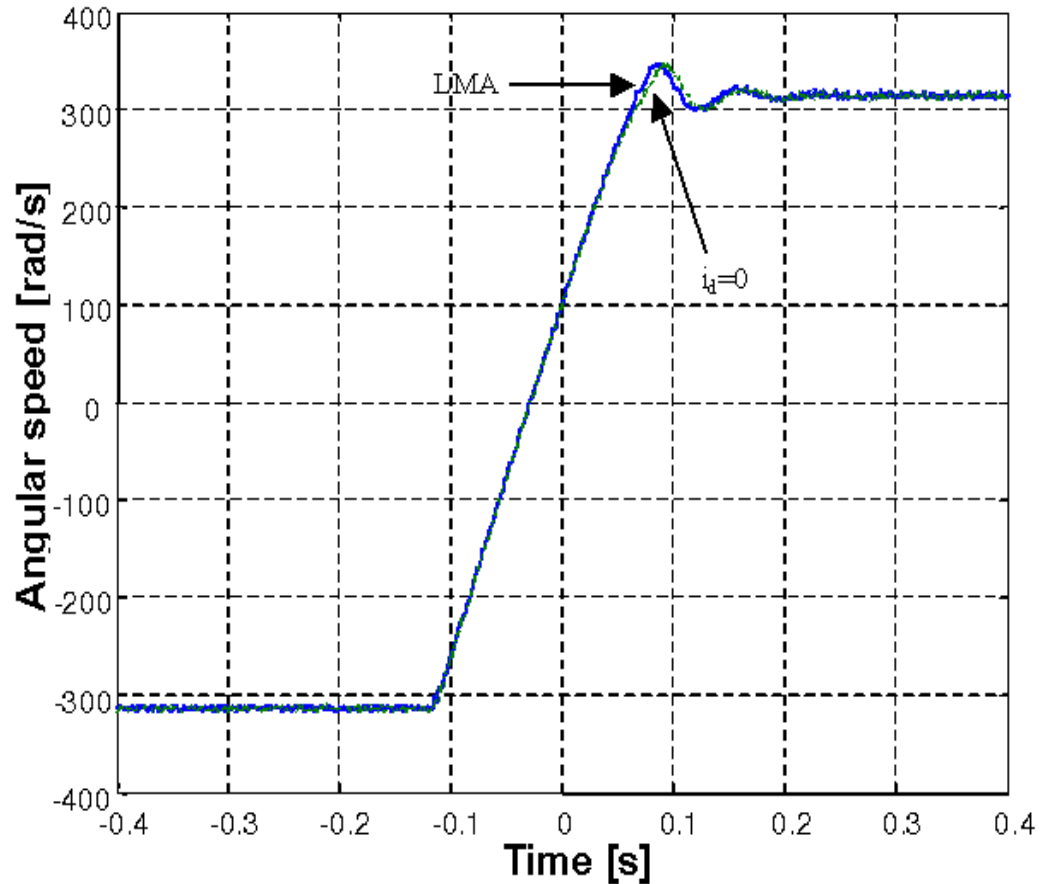


Achievable efficiency improvement due to LMA (referred to the traditional control approach) versus the load torque at rated speed (4000 rpm).



Laboratory Test Results

Performance comparison of the dynamic performance, which are obtained by two different control strategies, of the PMSM motor drive during a speed reversal from -3000 to $+3000$ rpm (-314 to 314 rad/s). The traces are in practice quite overlapped.



18 November 2010
University of Palermo



1. Introduction
2. FEM analysis of a commercial IPMSM (IPMSM 1 used in the LMFOC)
3. Comparison of FEM results with measured ones
4. Improvement of IPMSM performances with high energy PM (IPMSM 2)
5. Improvement of IPMSM performances with high energy PM and a better rotor geometry (IPMSM 3).
6. FEM results and electro-mechanical characteristics comparisons
7. Conclusions



Object of Study (IPMSM 1)

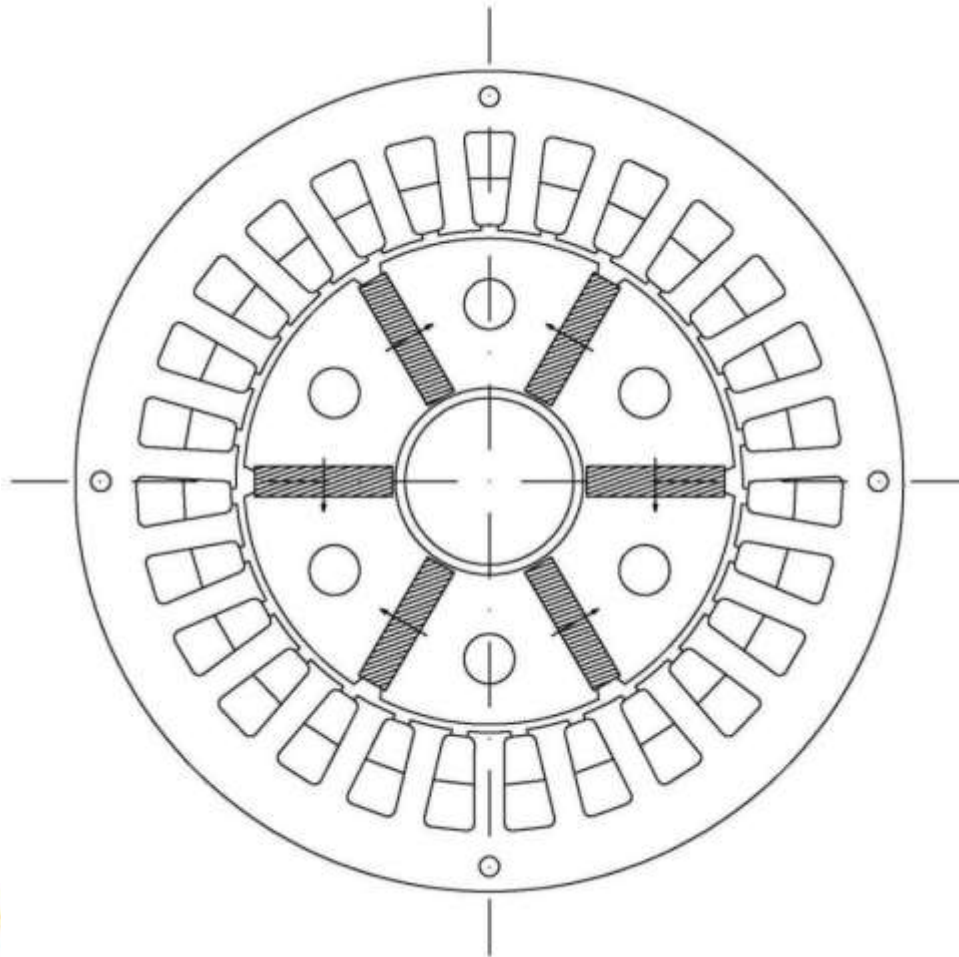


Table I: Rated values of IPMSM 1.

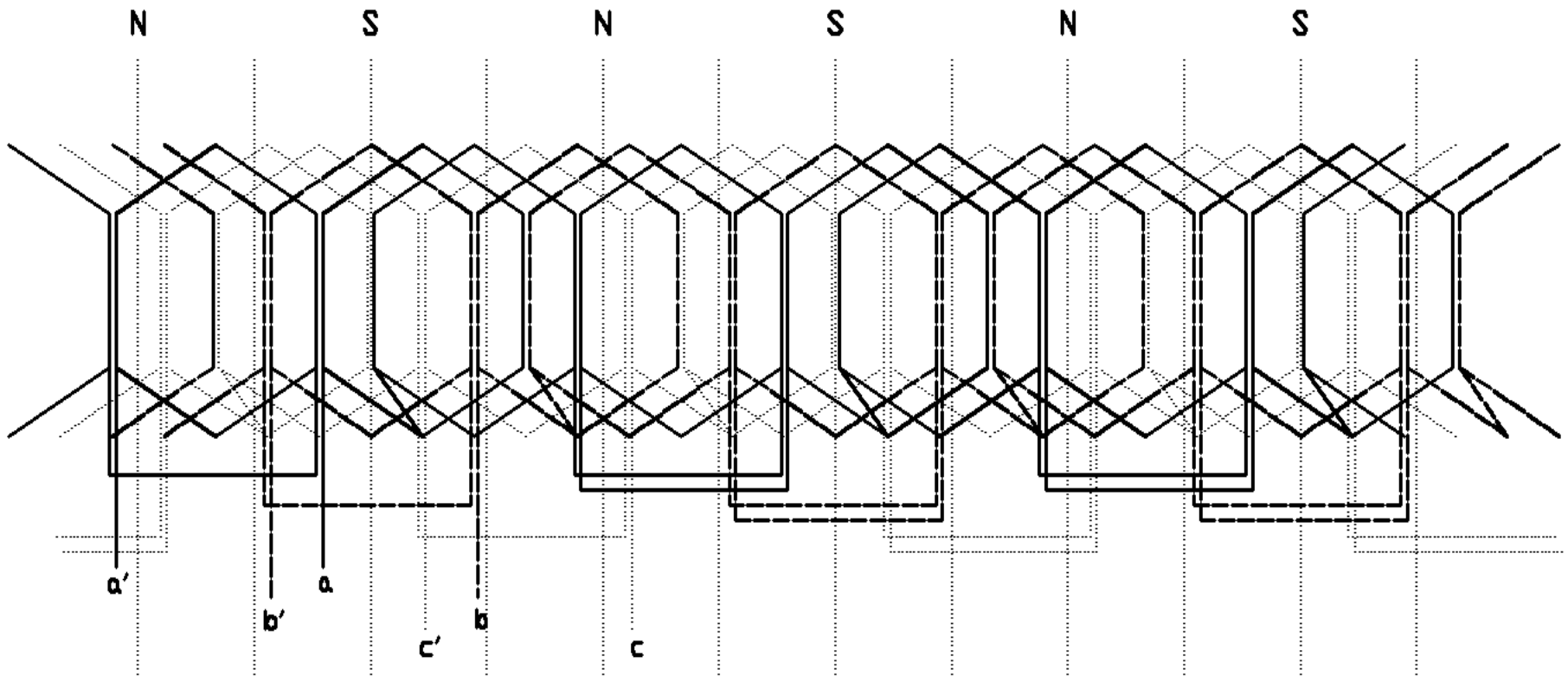
Item [unit]	Specification
Rated speed [rpm]	4000
Rated current [A]	3.6
Rated phase voltage [V]	77
Rated torque [Nm]	1.8
Number of poles	6
Stator resistance [Ω]	2.21
Direct axis inductance [mH]	9.7
Quadrature axis inductance [mH]	14.9
Mechanical loss torque [Nm]	0.04

Table II: Structure parameters of IPMSM1 and 2. All measurements are expressed in mm.

Item	Specification
External stator diameter	81
Internal stator diameter	49.6
External rotor diameter	48
Internal rotor diameter	18.46
Axial rotor length	59
PM width	13.45
PM thickness	3
Air-gap thickness	0.8
Slot depth	9.2
Slot mean width	4
Stator screw hole diameter	2
Rotor screw hole diameter	5
Shaft flux barrier thickness	1



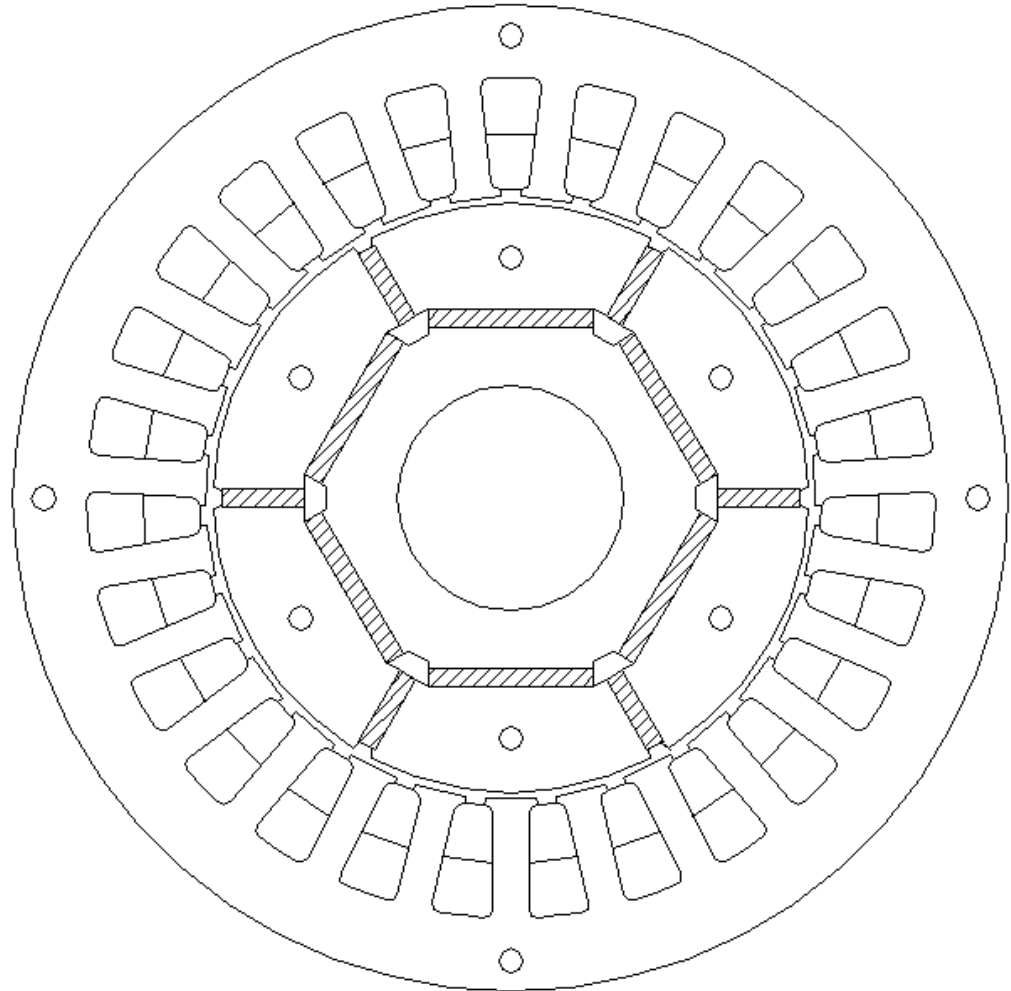
Object of Study (IPMSM 1)

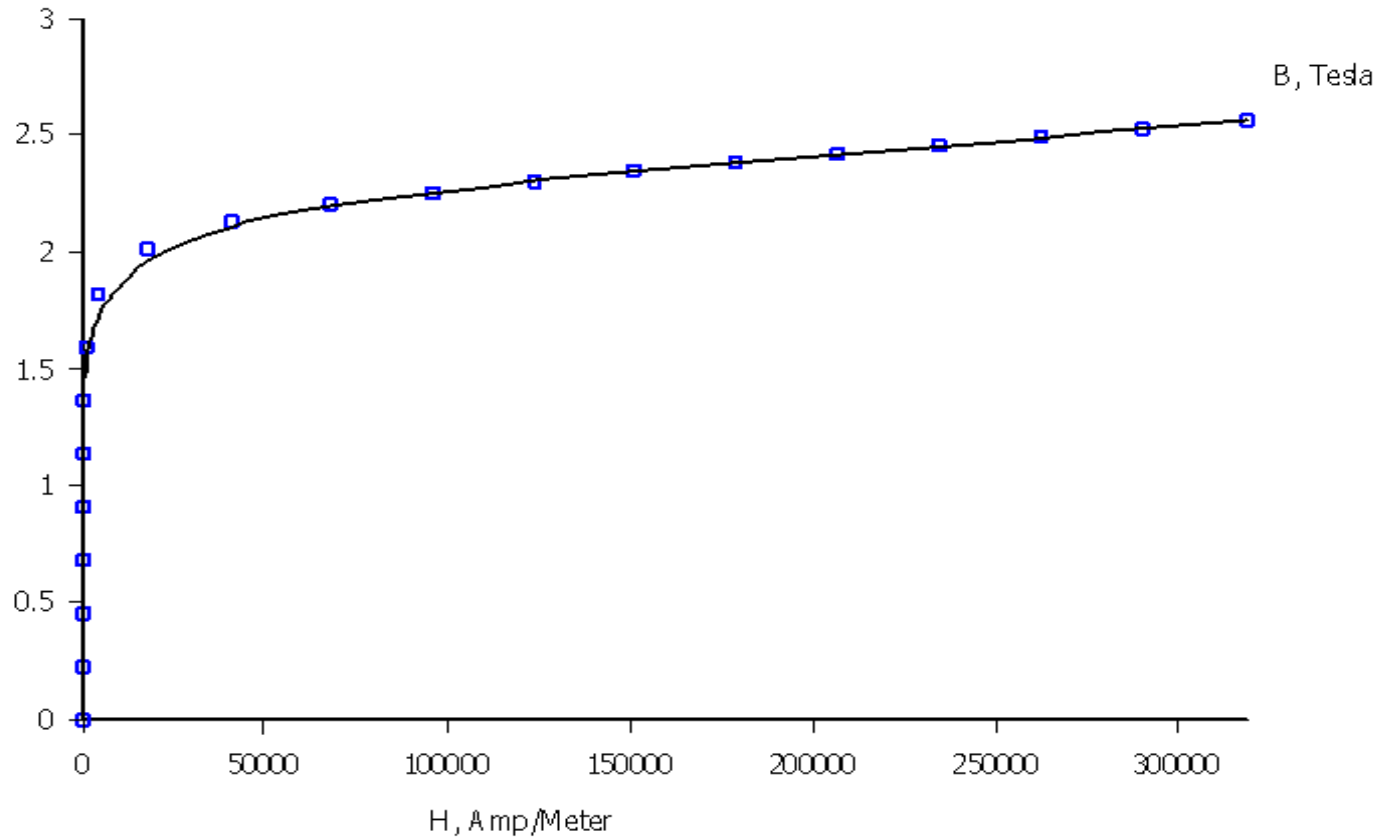


Winding type: $N=27$ slots, $p=3$ pole pairs, $m=3$ phases, $q=1.5$ slots per pole and per phase, double layer.



A new rotor geometry is here proposed.

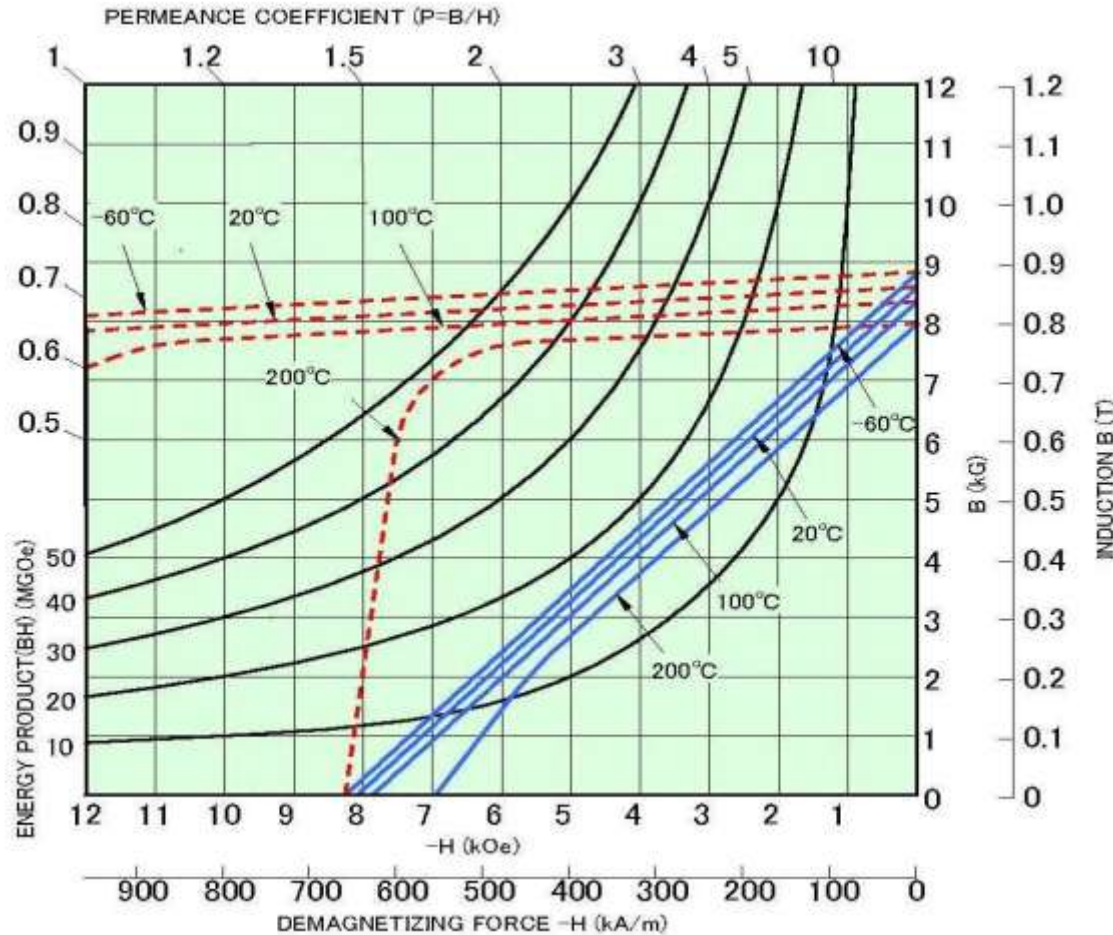




B-H curve for stator and rotor iron.



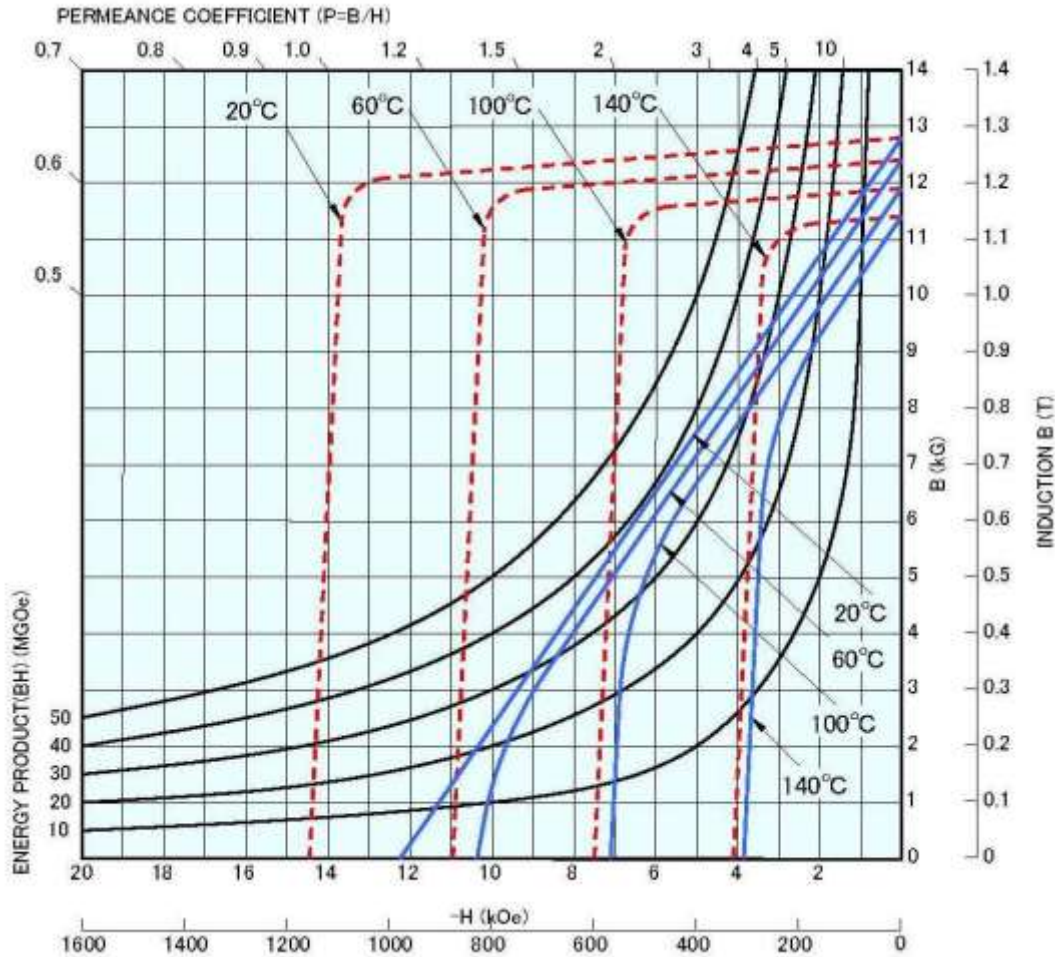
Material characteristics for IPMSM simulations



Characteristics of 18 MGO SmCo.



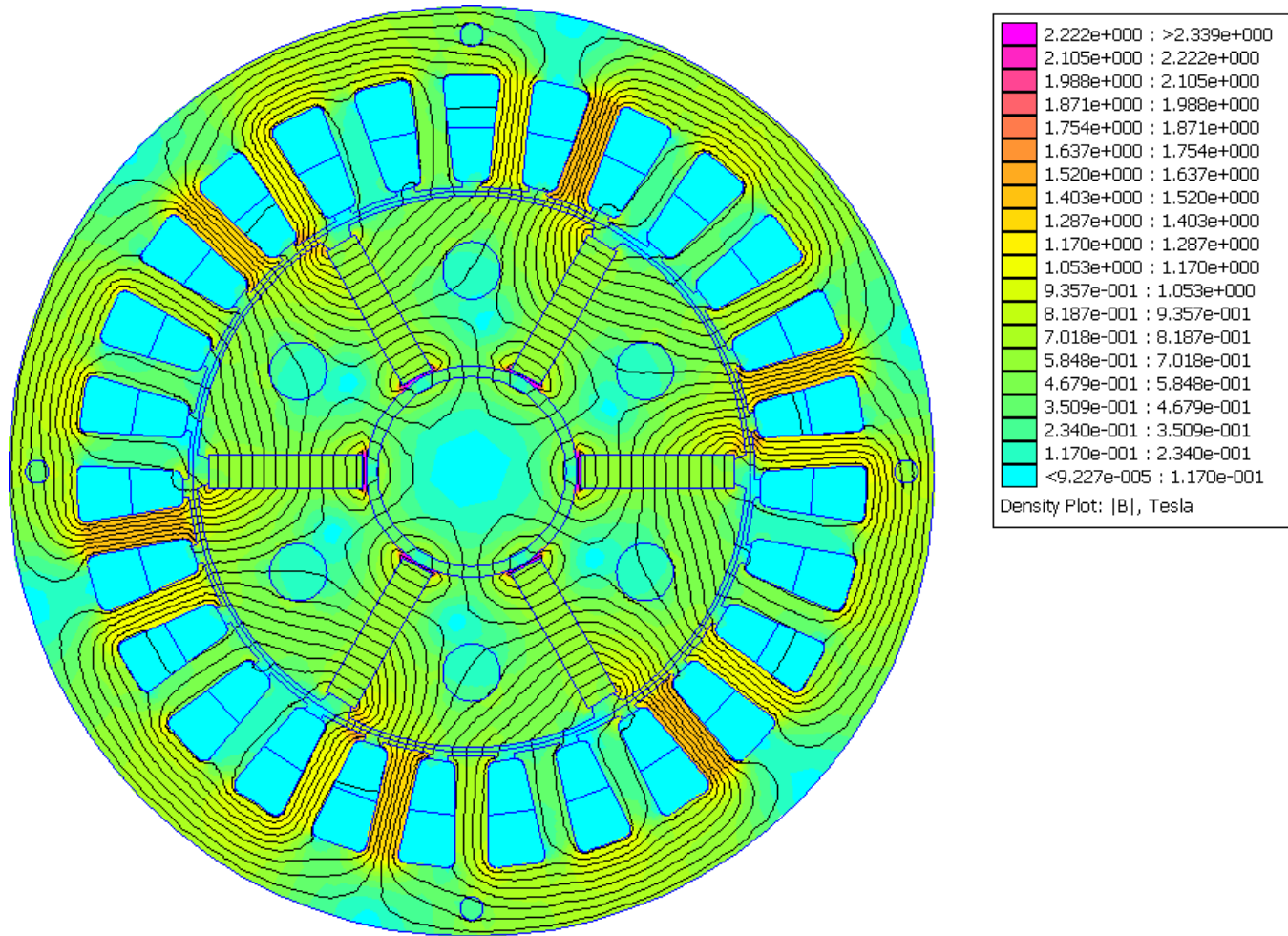
Material characteristics for IPMSM simulations

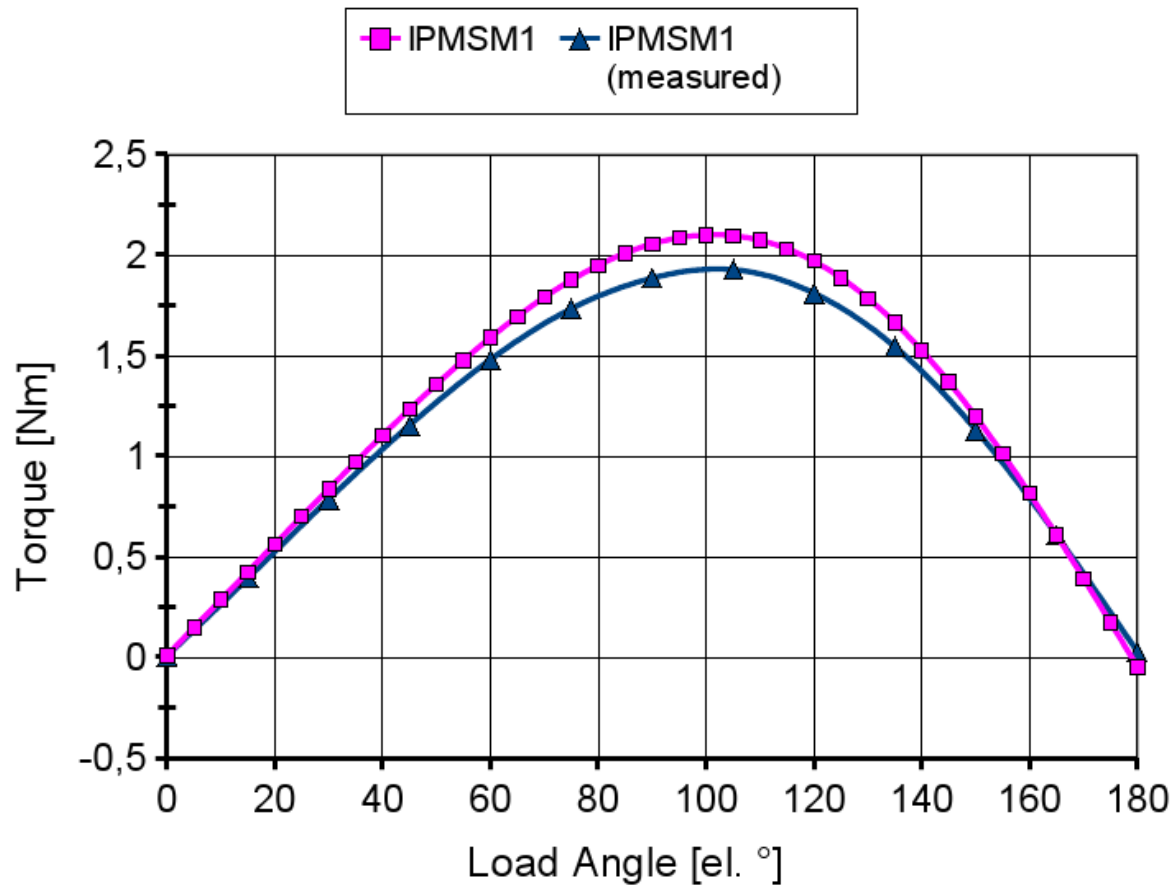


Characteristics of 40 MGO NeFeB.



FEM analysis



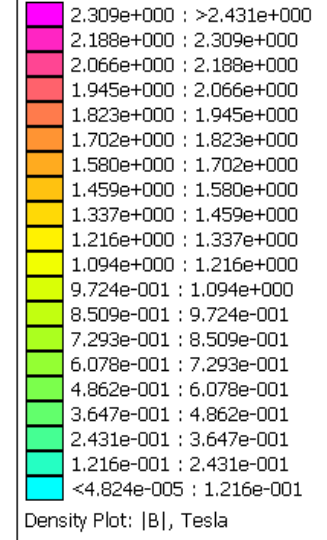
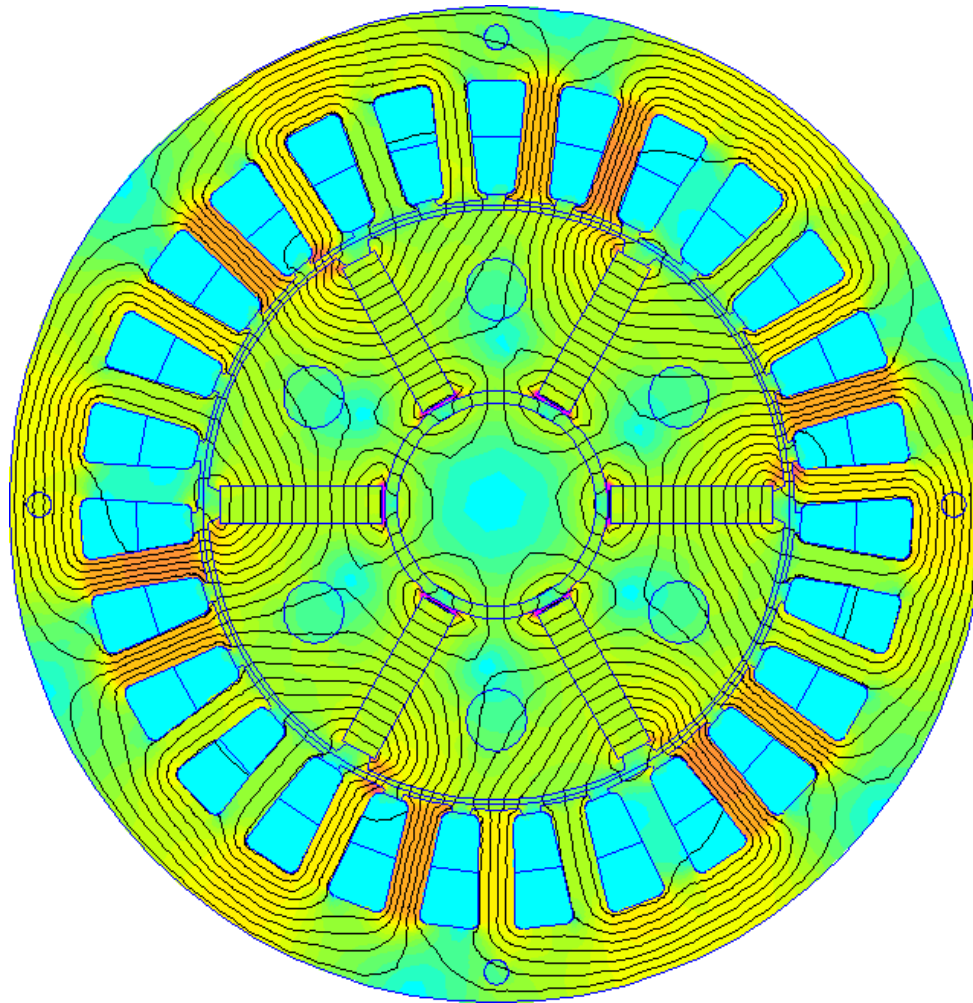


The developed torque is calculated by the Maxwell stress tensor

$$T_e = \frac{1}{\mu_0} \int_0^{2\pi} r^2 B_r B_\theta d\theta$$



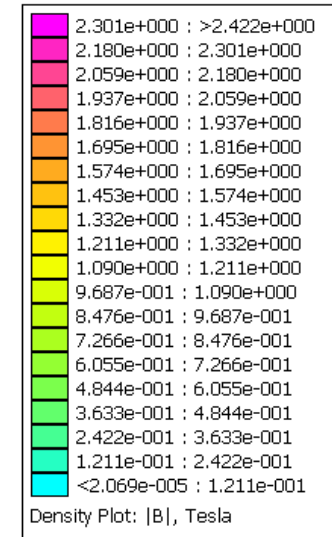
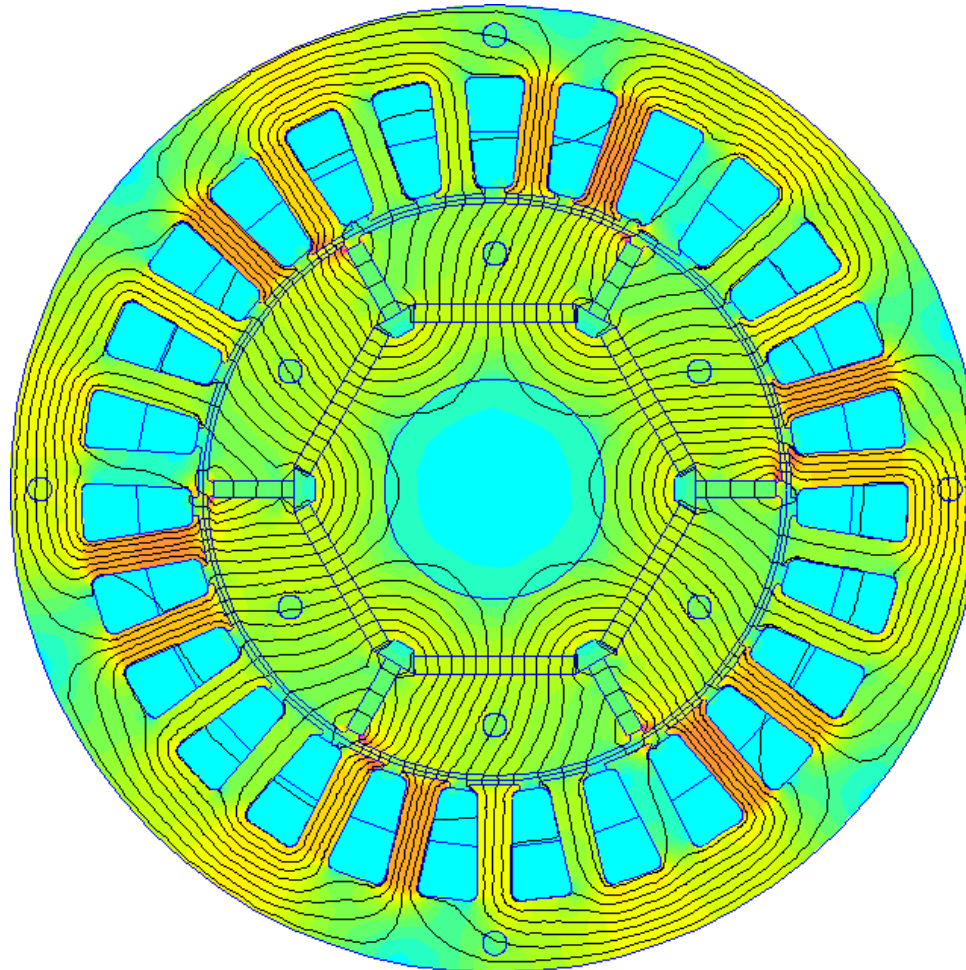
FEM analysis of IPMSM 2



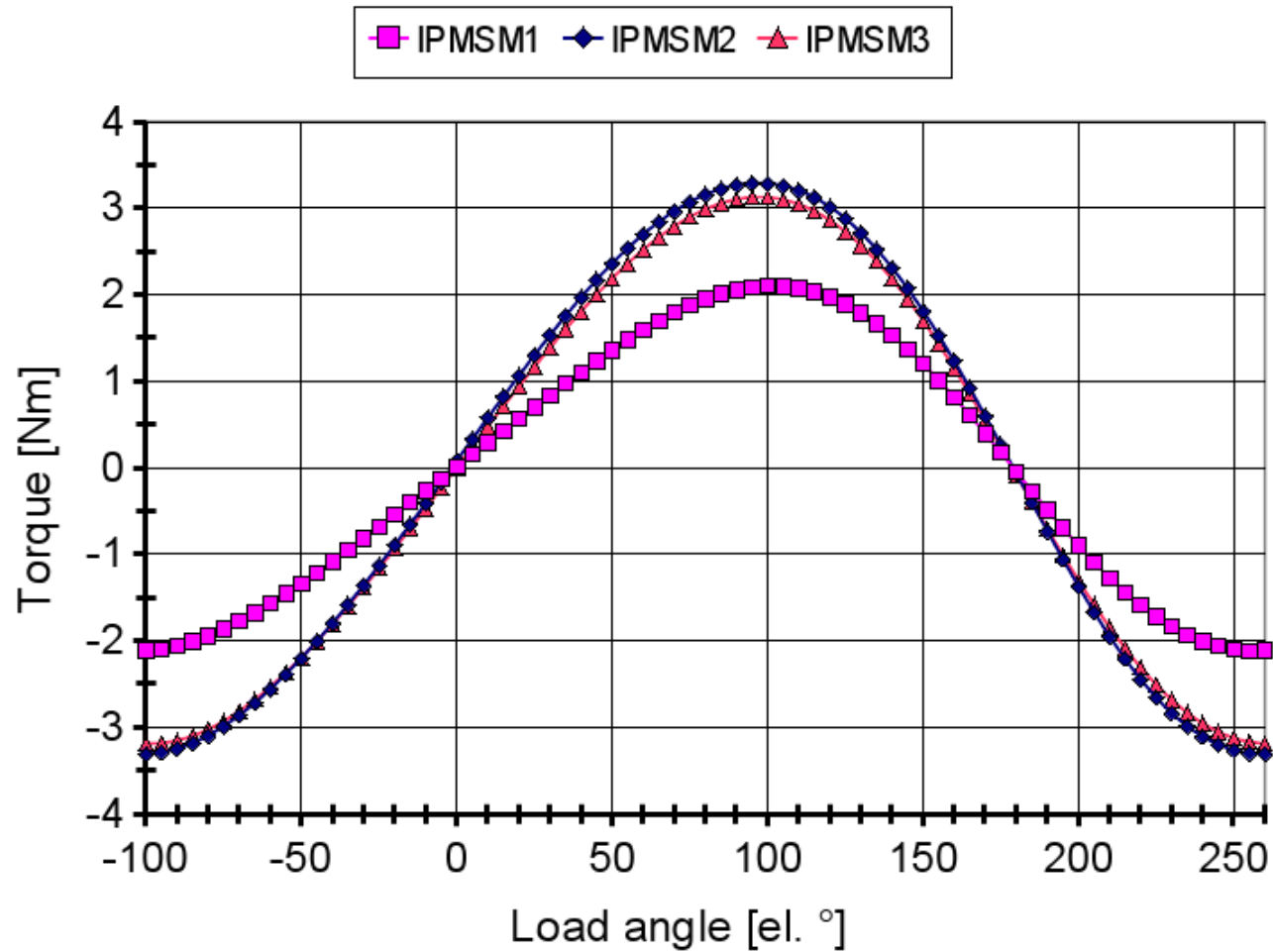
18 November 2010
University of Palermo



FEM analysis of IPMSM 3



Main results of FEM analysis



Main results of FEM analysis

Table III: Maximum developed torque and load angles at the rated current of 3.6 A.

Motor	T_x [Nm]	δ_x [el. °]
IPMSM1	2.10	100
IPMSM2	3.13	95
IPMSM3	3.29	95

Table V: Direct and quadrature inductances.

Motor	L_d [H]	L_q [H]	Saliency factor
IPMSM1	9.86	13.28	1.35
IPMSM2	9.86	13.28	1.35
IPMSM3	9.15	13.88	1.52

Table IV: Calculated pole fluxes of the simulated motors.

Motor	Flux [mWb]	Flux increment with respect to IPMSM1 [%]
IPMSM1	0.663979	—
IPMSM2	1.01483	52.84
IPMSM3	1.02002	53.62

Table VI: Performance indexes of the simulated motors.

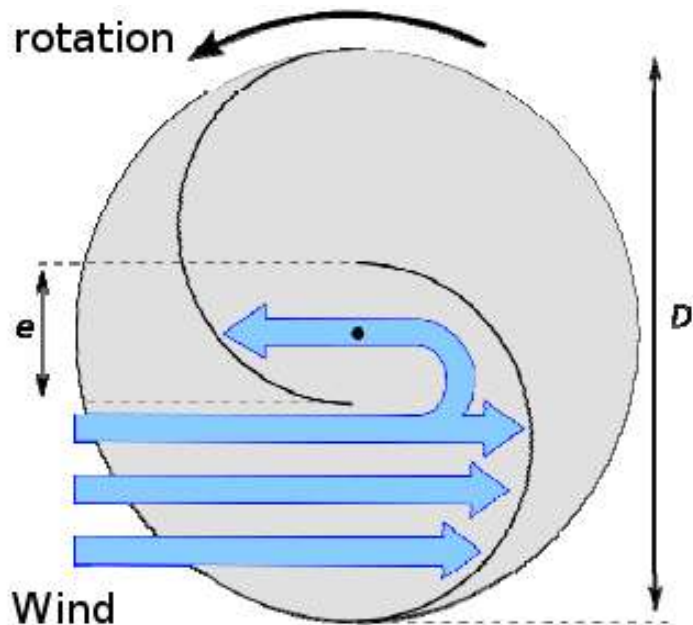
Motor	Max. torque [Nm]	Mass [kg]	Moment of inertia [kg m ²]	Torque/Moment of inertia [rad s ⁻²]	Torque/mass [Nm kg ⁻¹]
IPMSM1	2.10	2.26	0.23·10 ⁻³	9130	0.93
IPMSM2	3.13	2.25	0.22·10 ⁻³	14227	1.39
IPMSM3	3.29	2.26	0.23·10 ⁻³	14304	1.46

Table VII: Performance indexes of the simulated motors expressed in % with respect to IPMSM1 ones.

Motor	Max. torque	Mass	Moment of inertia	Torque /Moment of inertia	Torque /mass
IPMSM2	43.69	-0.44	-4.35	45.89	44.90
IPMSM3	51.35	0.00	0.00	52.83	52.04

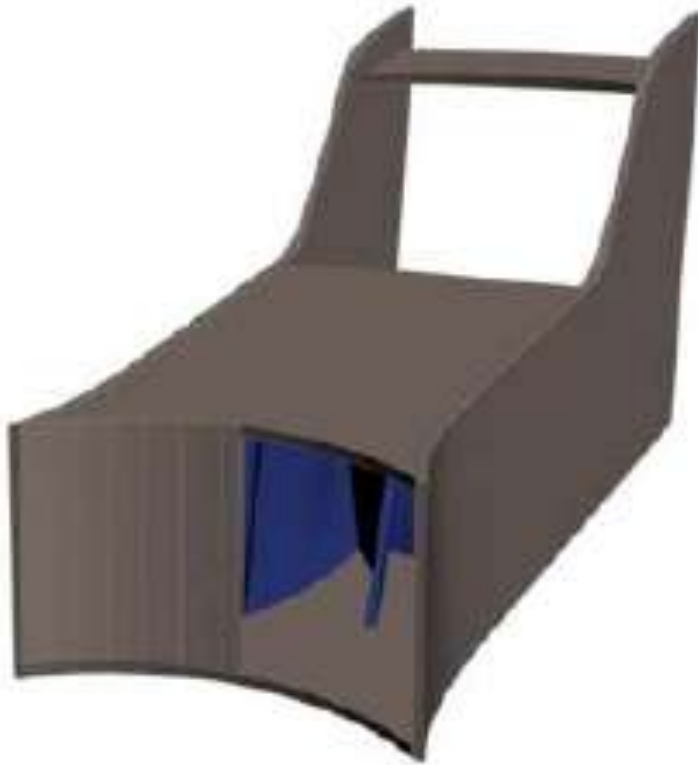


PMSGs in small wind turbine applications



Is it possible to apply the aforesaid criteria to small wind power generators?

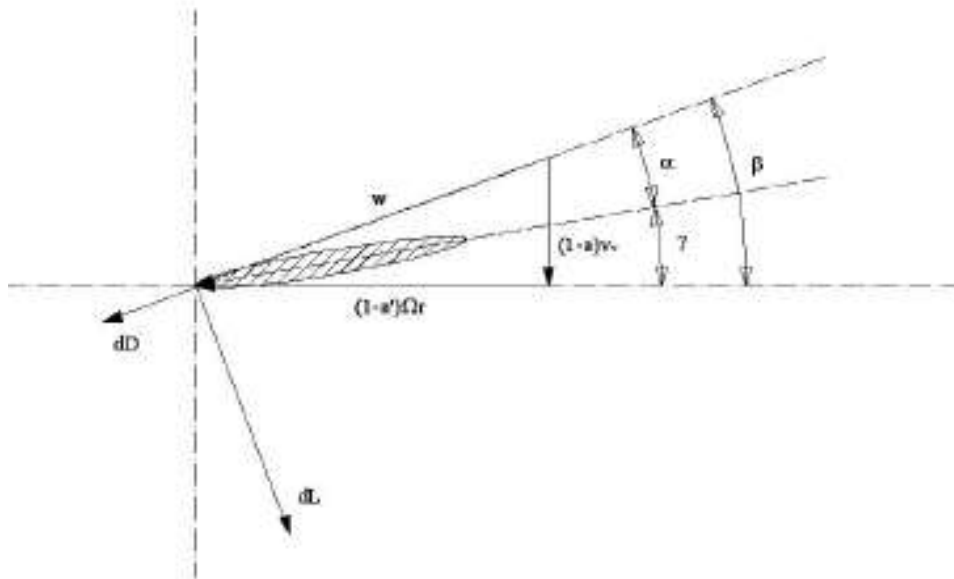




...by inserting a cover structure acting as a channelling-case with the aim to favour the wind flux flow within the turbine and to reduce the aerodynamic resistance caused by the wind flow opposing the convex surface of the rotor blades.



Aerodynamic design model.



$$\left\{ \begin{array}{l} w^2 = (1-a)^2 v_v^2 + (1-a')^2 (r\Omega)^2 \\ \beta = \arctan \frac{(1-a)v_v}{(1-a')(r\Omega)} \\ \alpha = \beta - \gamma \\ dD = \frac{1}{2} C_D \rho w^2 c dr \\ dL = \frac{1}{2} C_L \rho w^2 c dr \\ dT_m = (dL \sin \beta - dD \cos \beta) r \\ T_m = \int_{R_{min}}^{R_{max}} N dT_m = \\ = N \int_{R_{min}}^{R_{max}} (dL \sin \beta - dD \cos \beta) r \end{array} \right.$$

C_D and C_L depend on the chosen blade profile.



Design of the Wind Turbine



Inner side of the wind turbine

Design characteristics

Data	Value	Unit
Rated power at 12 m/s	2	kW
Power at 7 m/s	250	W
Cut-in speed	4	m/s
Cut-out speed	17	m/s
Max rot. speed	180	rpm
Gear box	Not present	
Weight	95	kg



Design Procedure of the PMSG



Fundamental design parameters

Fundamental design parameters	{	Rated power (P):	2 kW
		Rotational speed (Ω):	180 rpm

The geometrical dimensions are defined as a function of the wind turbine characteristics and the parameter *specific torque* “k”.

This parameter is extrapolated from old studies and from practice.

(the specific torque is the torque for each pole pair and for a unit of axial length of a MP machine)

$$k = \frac{C}{p \cdot l} \left[\frac{Nm}{mm} \right]$$




Rated power

$$C = \frac{P \cdot 60}{n \cdot 2 \cdot \pi} [Nm]$$

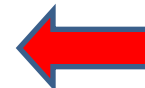


Design Procedure of the PMSG

Ω [giri/1']	f [Hz]	p
180	50	16
180	60	20
180	63	21
180	70	23




$$l = \frac{C}{k \cdot p} \quad [mm]$$
 Generator axial length


 For winding design reasons the number of pole pair must a multiple of 3 (base winding)

By means of the pole pitch τ the air gap average circumference " C_t " is calculated:

$$C_t = 2 \cdot \tau \cdot p$$


$$N = \frac{C_t}{\tau_{slot}}$$
 Number of stator slots



$$q = \frac{N}{2 \cdot p \cdot m}$$
 Number of slots per pole and per phase

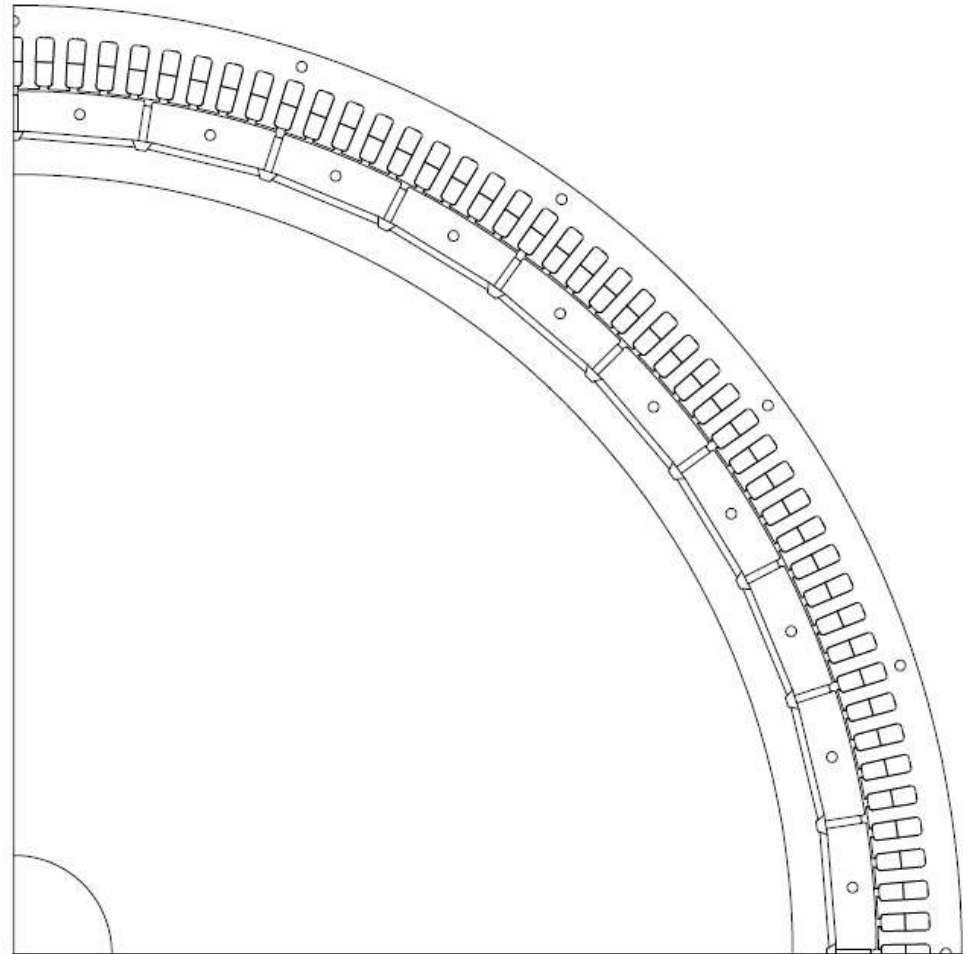


Design Procedure of the PMSG

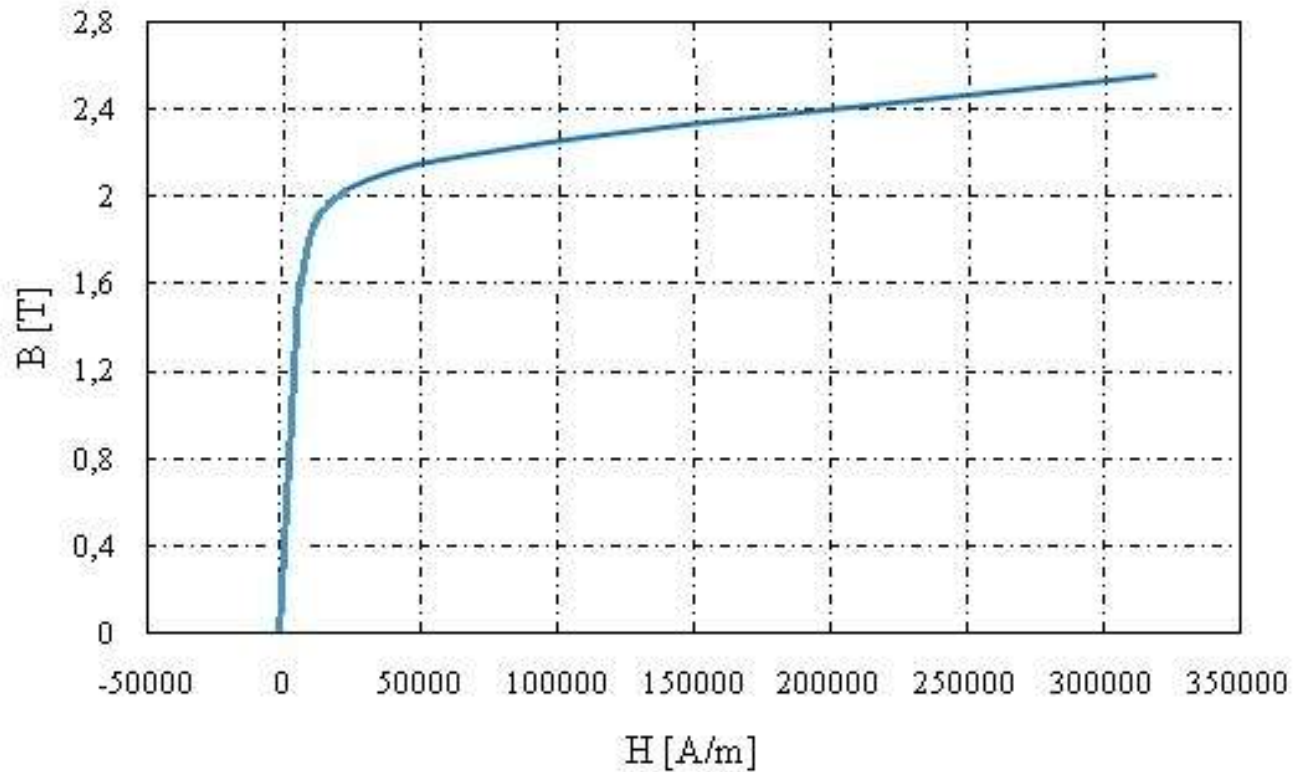
Rated values of the PMSG.

Data	Value	Unit
Rated power	2	kW
Number of poles pairs	21	
Rated frequency	63	Hz
Rated speed	180	rpm
Rated voltage	253	V
Rated curren	25,2	A
Nr. of slots per pole and phase	1,5	

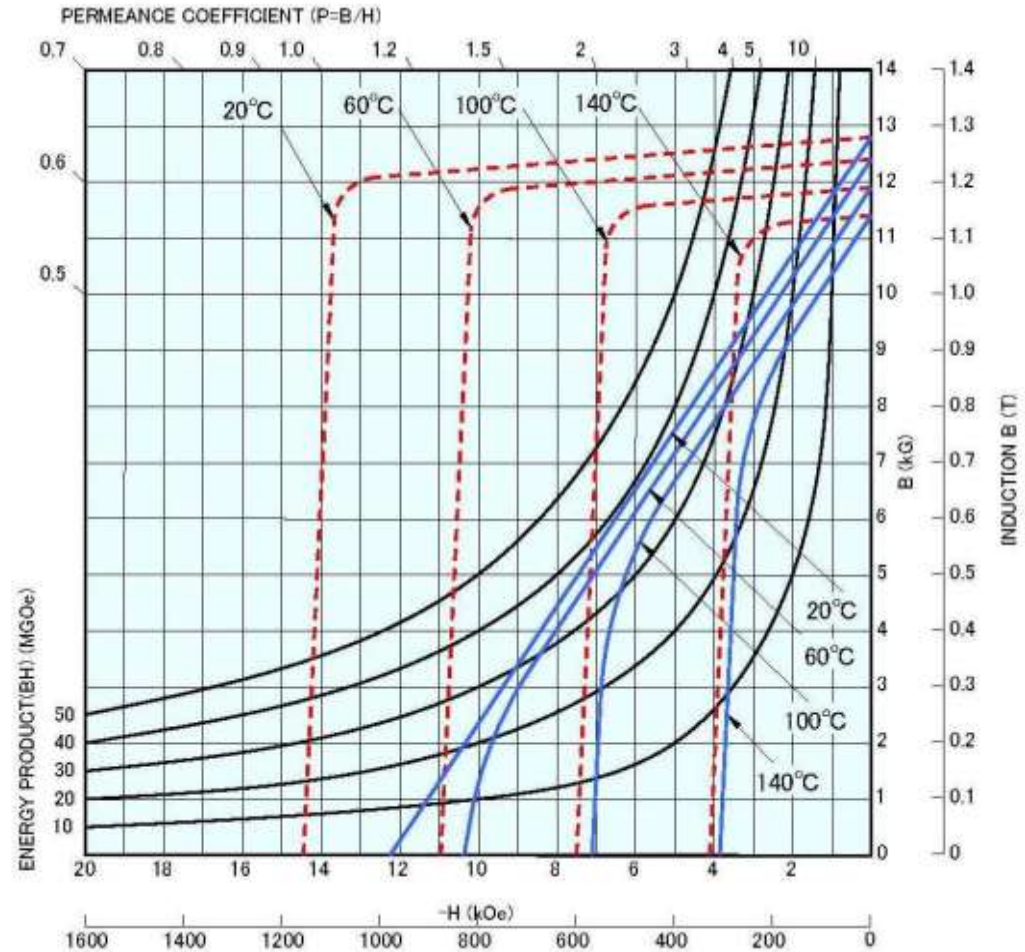
7 parallel connected base windings ($p=3$) are foreseen, each of one with a rated current of 3.6 A



Magnetic characteristic of the laminated iron (0.5 mm).



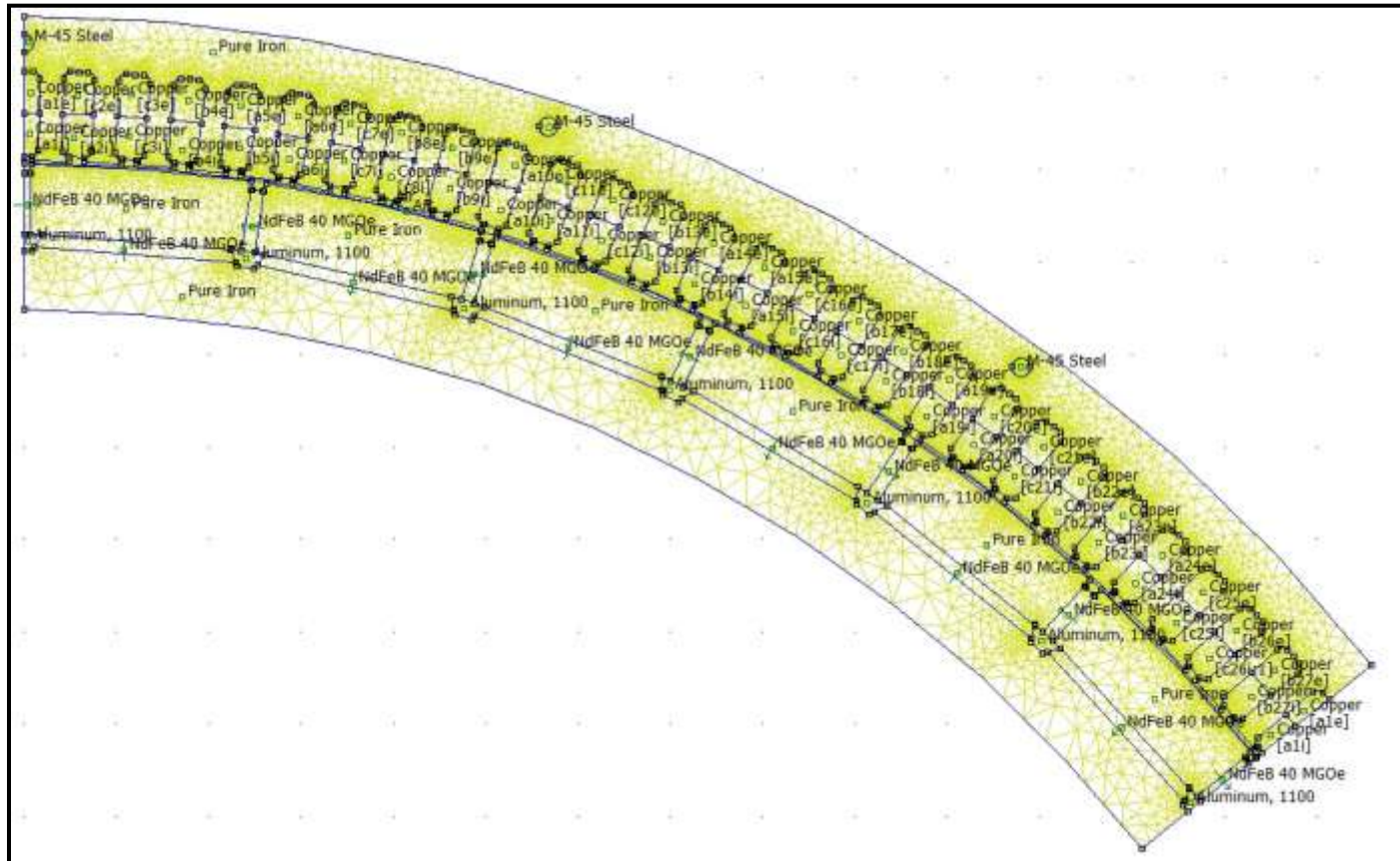
Characteristics of
the NeFeB
permanent magnets
(40 MGOe)



18 November 2010
University of Palermo



FEM meshing, materials and boundary condition definitions.



18 November 2010
University of Palermo



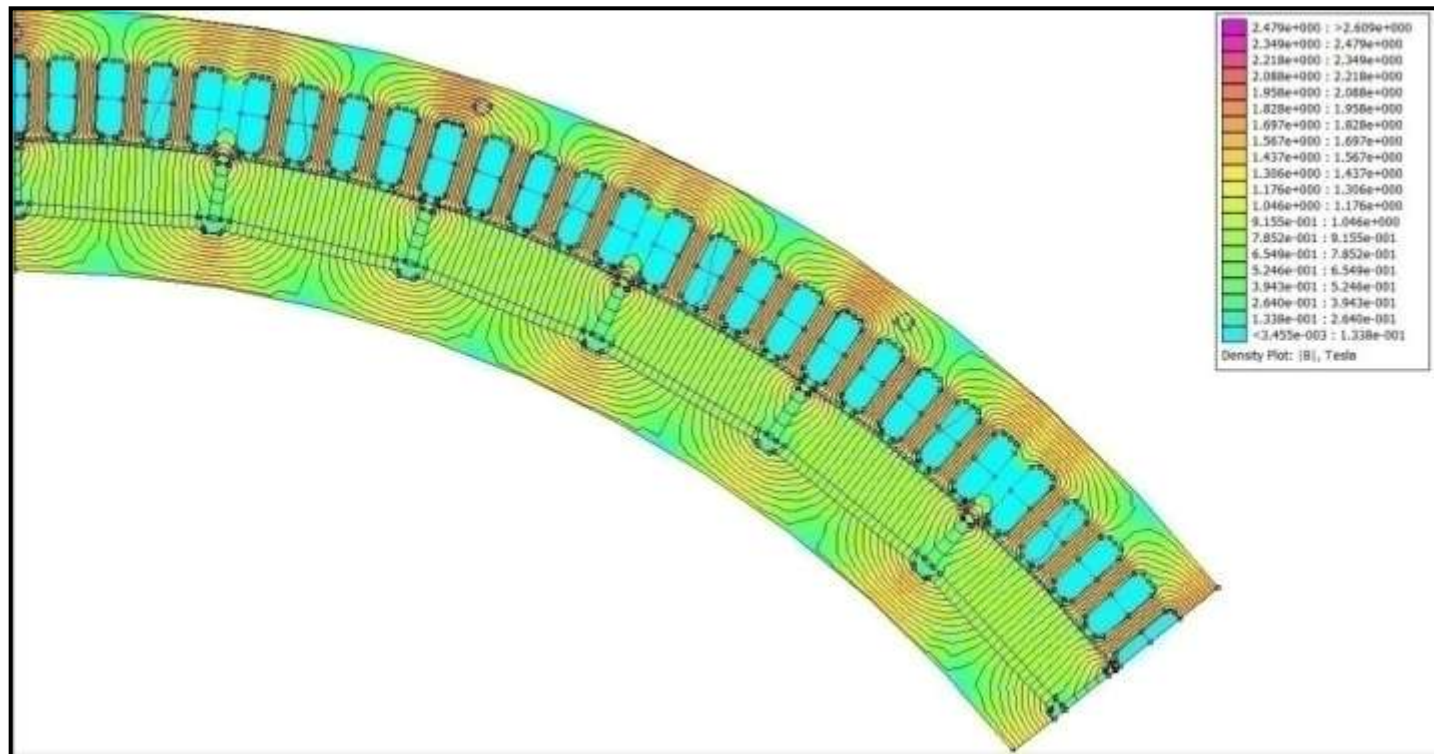
Two conditions were taken into account in the design:

1. No load condition

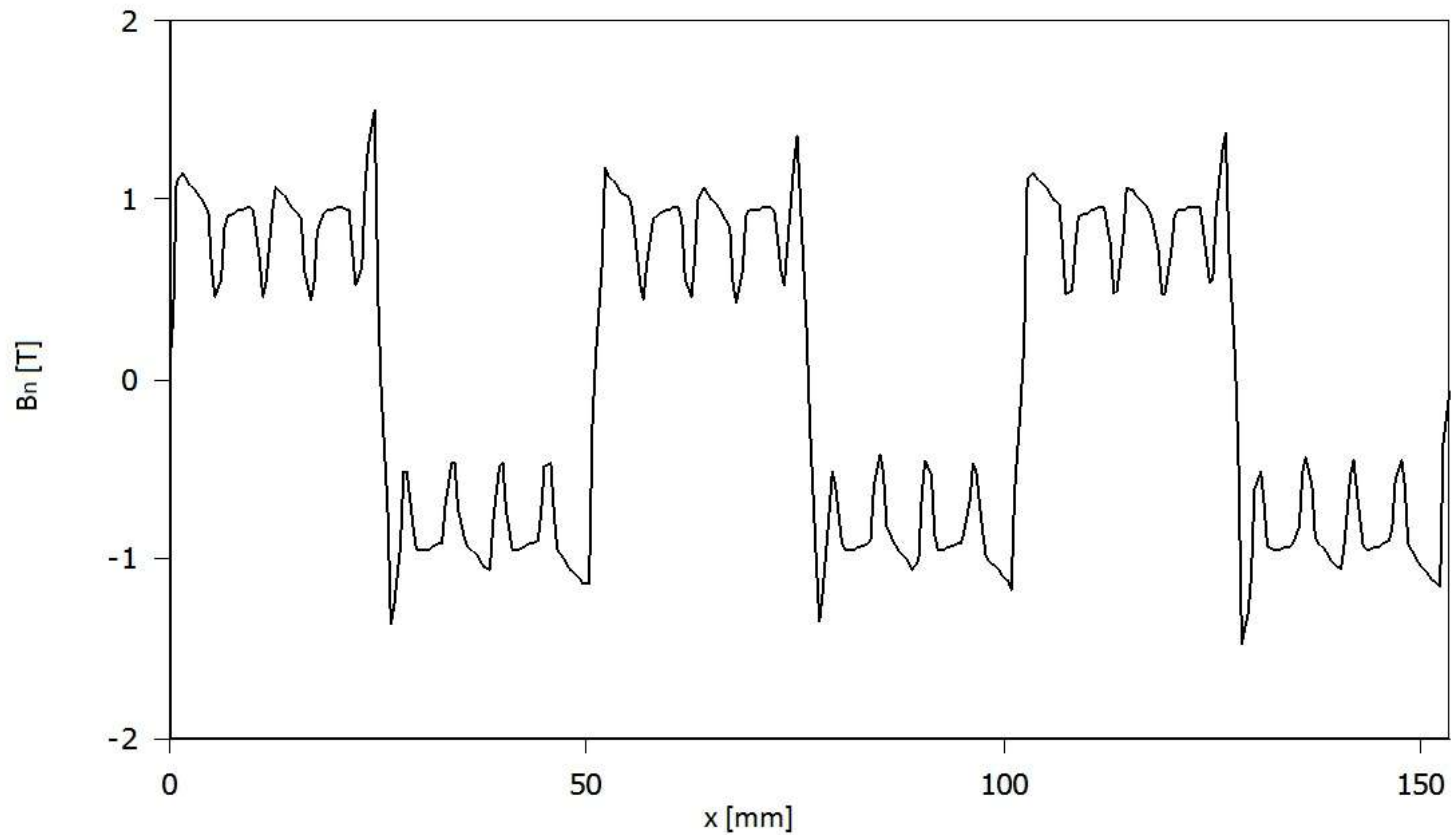
1. Full load condition at P.F=1



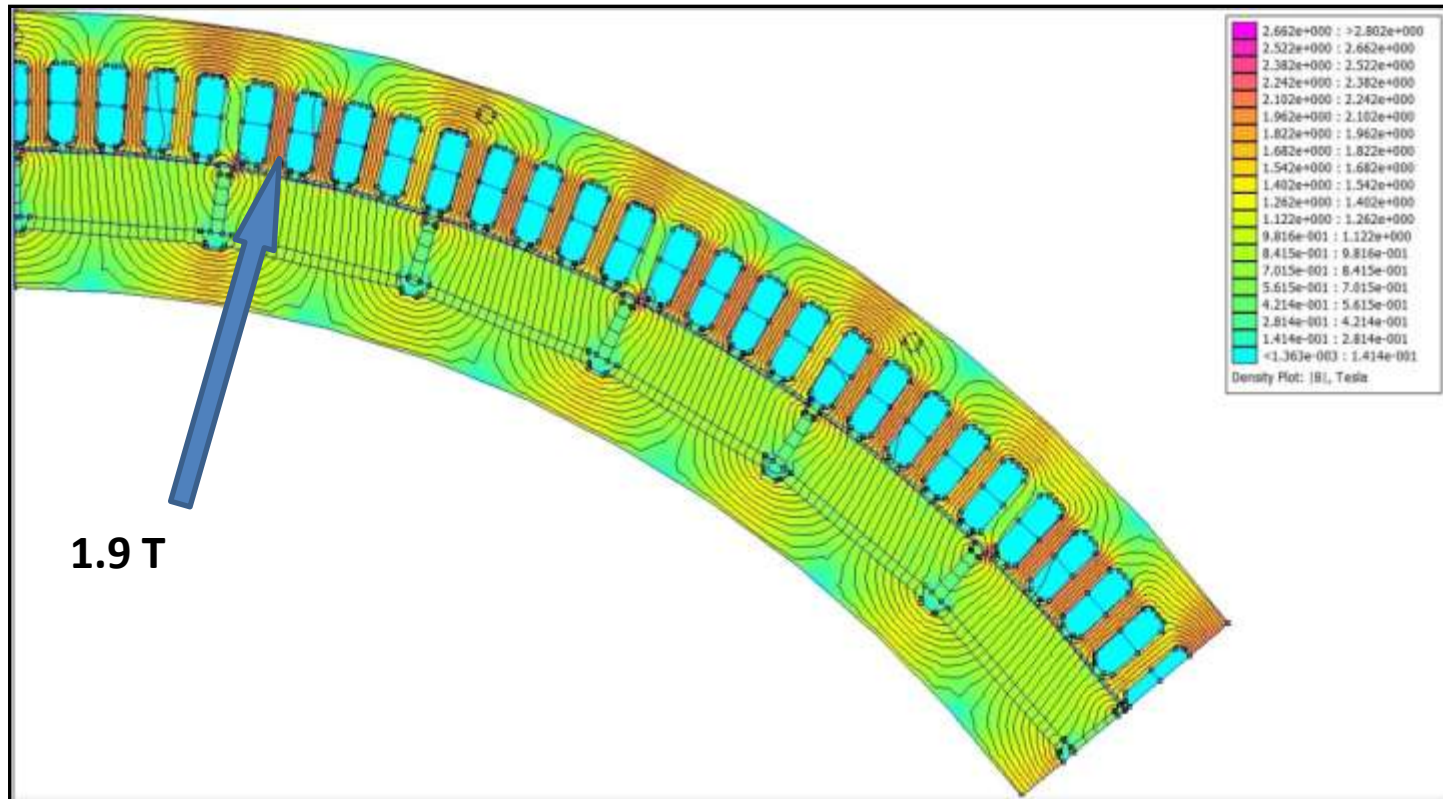
Flux density plot at no load



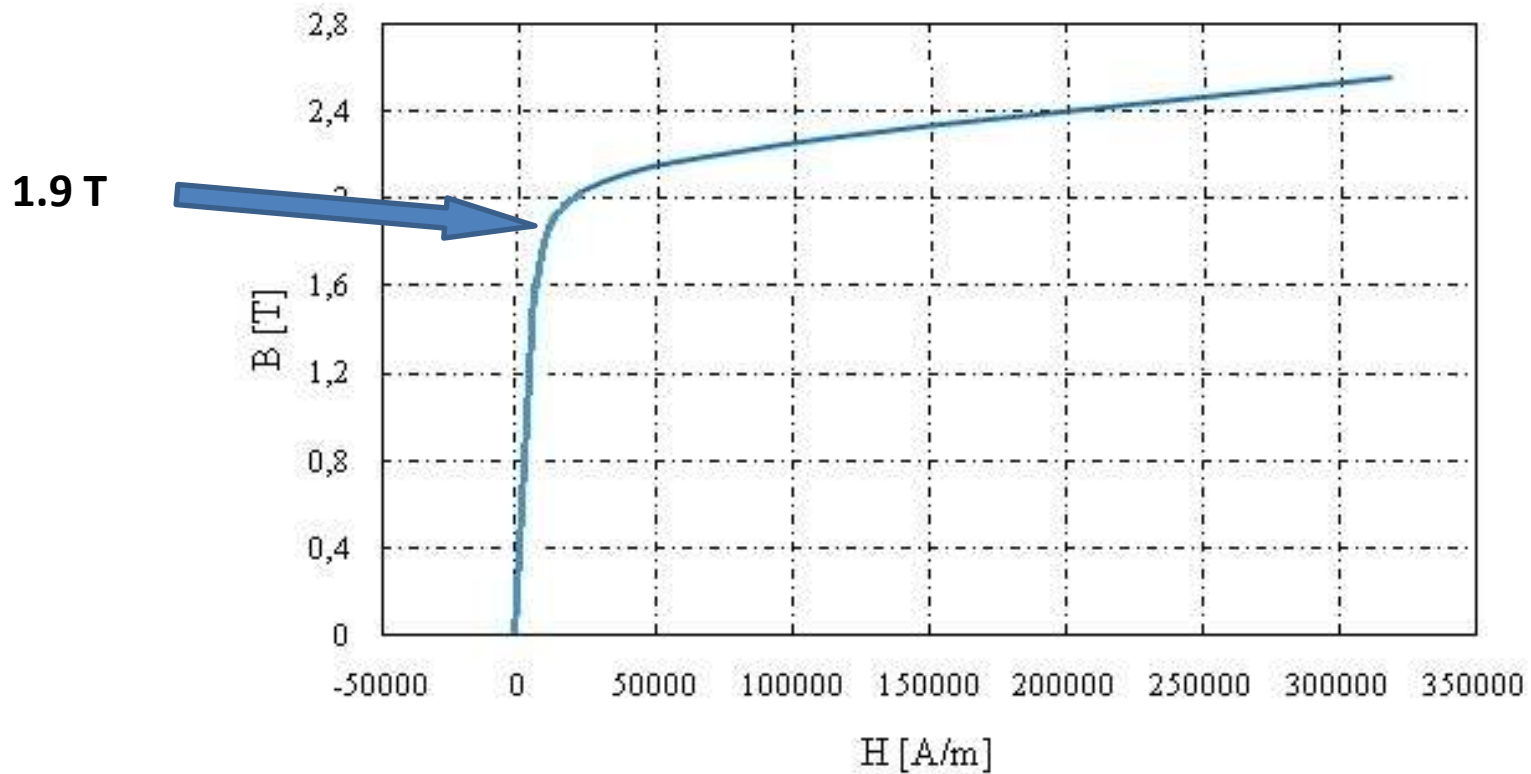
Air gap radial component of flux density at no load



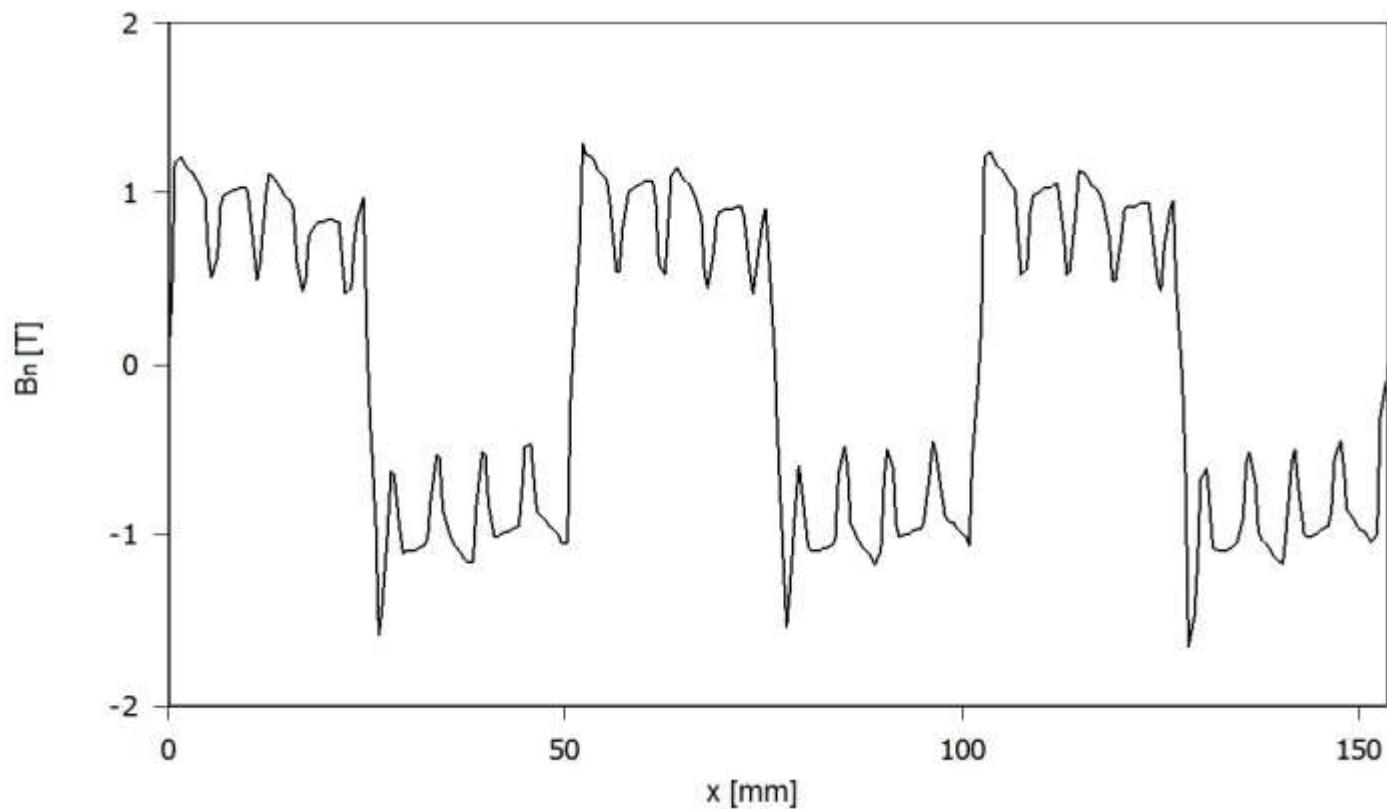
Flux density plot at full load.

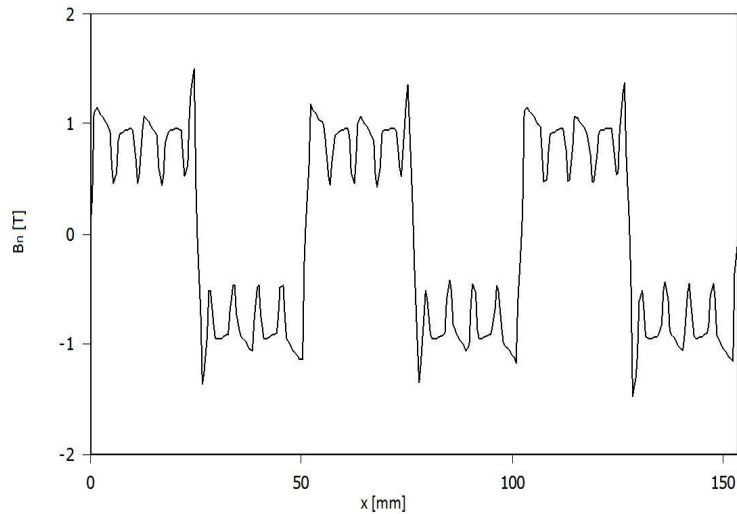


Flux density plot at full load. Tooth density is 1.9 T causing no magnetic saturation.



Air gap radial component of flux density at full load



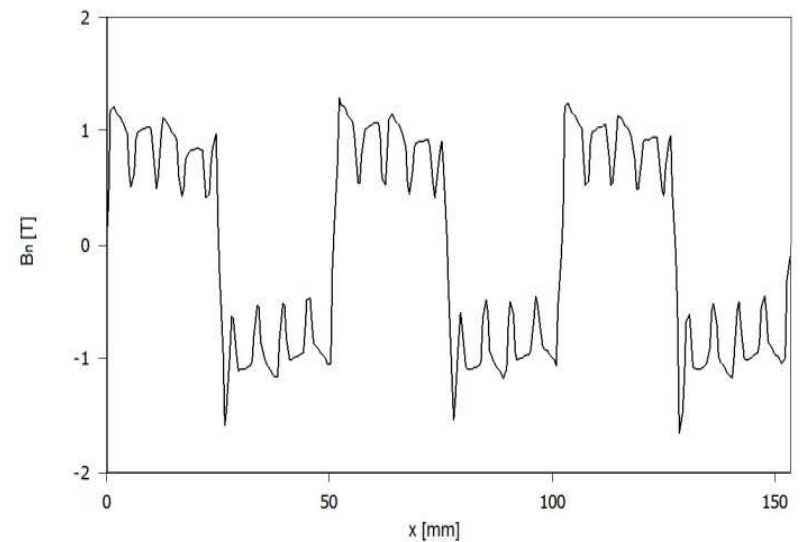


No-load

Harmonic content of flux density is almost the same as at no-load. Hence armature reaction is negligible.

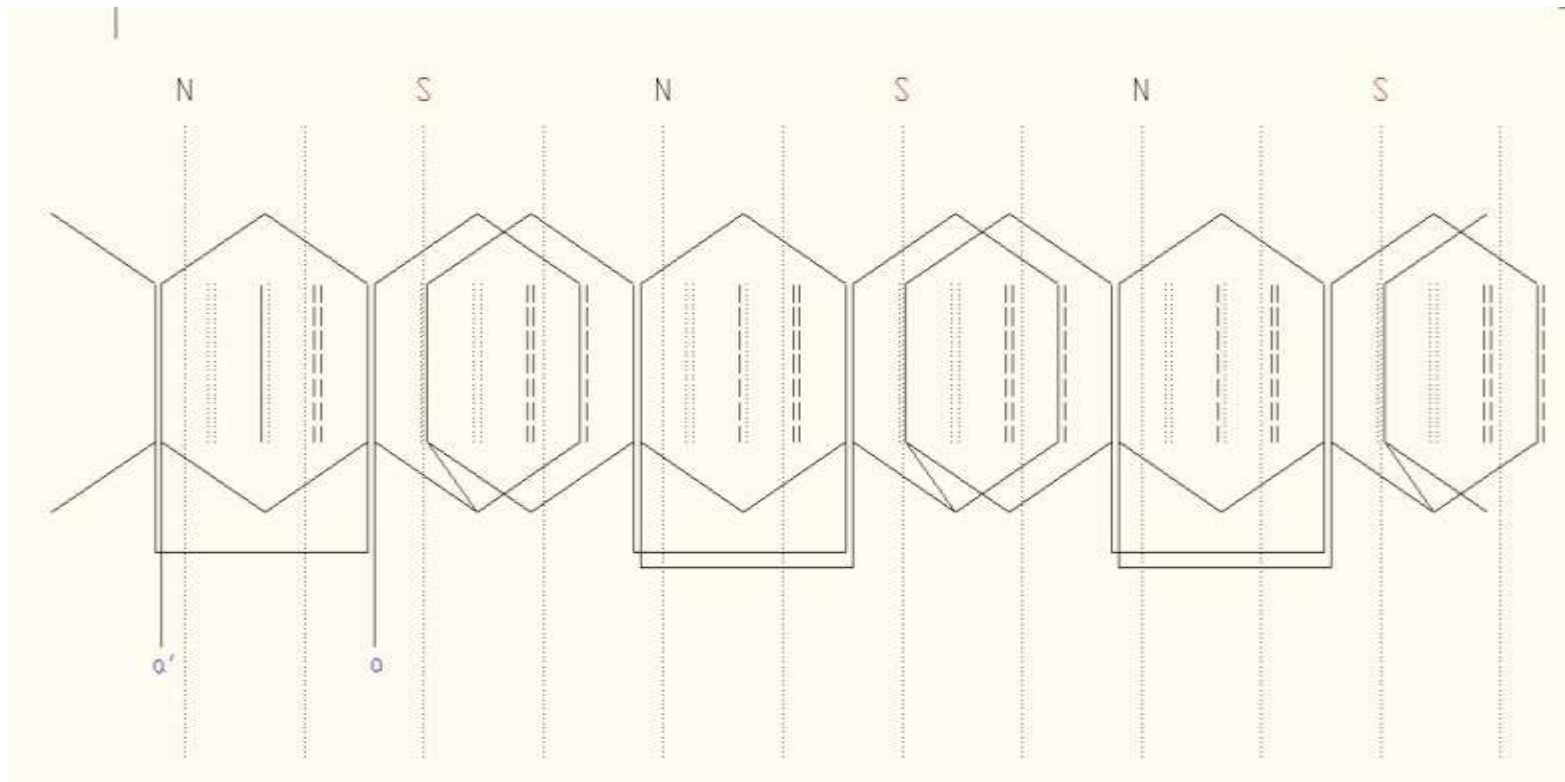
Effect of armature reaction.

Full load



PMSG Design Verification

Base winding diagram for $p=3$ poles $q=1.5$ slots/pole phase



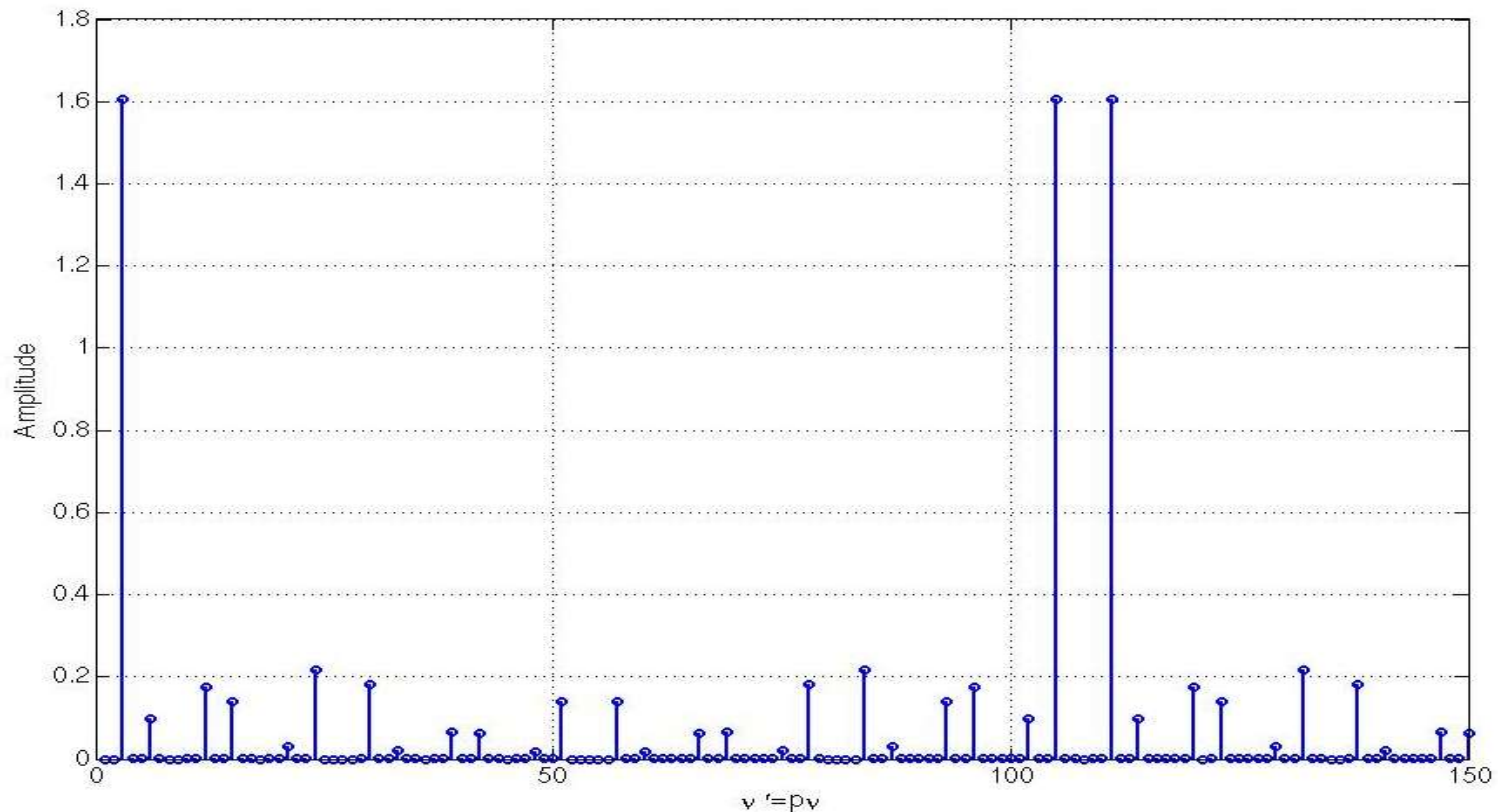
Expression of the 1-st harmonic component of the induced e.m.f.

$$E_{em} = 2,22 q 2p N_s f f_w \varphi_{PM}$$



PMSG Design Verification

Winding factor spectrum (including distribution, pith shortening, pole shoes skewing and phase-to-phase connection factors). $q=1.5$ slots/pole phase

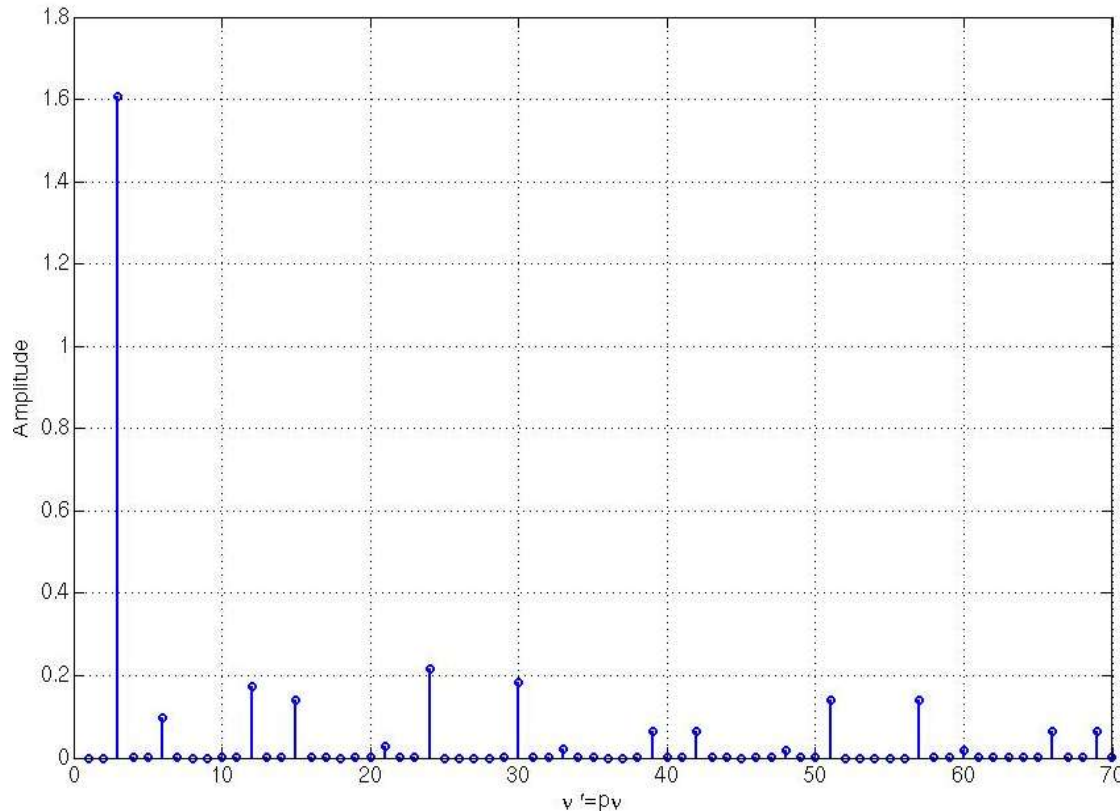


18 November 2010
University of Palermo



PMSG Design Verification

Winding factor spectrum (including distribution, pith shortening, pole shoes skewing and phase-to-phase connection factors). $q=1.5$ slots/pole phase



Data	Value	Unit
Pole flux	6,26	mWb
1 st harmonic winding factor	1,6	
Nr. of conductors in a slot	20	
Nr. of slots per pole and phase	1,5	

18 November 2010
University of Palermo



Quantities

Values

Stator external diameter	733,38 [mm]
Stator bore	341,98 [mm]
Rotor external diameter	341,18 [mm]
Rotor iron depth	37 [mm]
Axial machine length	265,92 [mm]
Air gap length	0,4 [mm]
Slot depth	9,21 [mm]
Slot average wideness	3,27 [mm]
Stator diameter threads	2 [mm]
Rated speed	180 [giri/1']
Rated current	25,2 [A]
Rated voltage	252,8 [V]
Rated electromagnetic torque	106,10 [Nm]
Number of poles	42

18 November 2010
University of Palermo



Conclusions. 1



A dynamic model of the PMSM, which takes into account the iron and copper losses, and a “loss-model” control strategy have been presented.

In particular, it has been verified by laboratory tests that controlling the stator current space vector can minimize the controllable electrical losses occurring in a PMSM drive, consisting of the fundamental copper and iron losses.

Such a control strategy, accounting for both the instantaneous speed values and the load torque condition, uses the combined effects of the field weakening and the exploitation of the reluctance torque.

The loss minimization technique here reported is very flexible and simple to implement because only requires the knowledge of the common motor parameters.

The main results of the laboratory tests carried out demonstrated how, in comparison with more traditional control methods, the loss minimization algorithm



Conclusions. 2



Starting from a commercial PMSM, whose parameters and machine ratings are known, the following results were obtained:

- 1) a rotor optimization with an increase of performance in terms of torque;
- 2) a reduced rotor leakage flux;
- 3) a reduction in PM material quantity of about 25%;
- 4) an increase of the motoring torque of about 50%.

The improvement has been achieved with limited changes in the rotor geometry, without varying the stator iron core structure and windings

To optimize the rotor configuration a steady-state performance comparison have been provided. The comparison has been performed by using a FEM-based software.

The FEM analysis has been validated by comparing the results with the torque-load angle characteristics measured on a real motor by means of a test bench.



As regards the the small wind turbine application the improvements consist mainly in:

- 1) the introduction of a channelling-case capable to increase the efficiency of the wind turbine;**
- 2) the possibility to work at low rotational speeds; the reduction of noise during service.**

The PMSG improvements consists in the:

- 1) reduction of the harmonic content in the induced emf;**
- 2) reduction of the weight of the magnetic structure (optimization and use of high energy Pms).**



In the future tests on the wind turbine and on the PMSG will be carried out for the experimental validation of the proposed design elements.

This wind generation system for local DoS applications opens new scenarios towards the penetration in the market of energy management of connected household appliances integrated with combined wind, photovoltaic and solar-thermal systems.



Thank you for your kind attention

